Surfactant free microemulsions: possible applications for solubilisation and extraction of hydrophobic components

Jurko, Lucija

UNIVERSITY OF SPLIT

FACULTY OF CHEMISTRY AND TECHNOLOGY

SURFACTANT-FREE MICROEMULSIONS: POSSIBLE APPLICATIONS FOR SOLUBILISATION AND EXTRACTION OF HYDROPHOBIC COMPONENTS

DIPLOMA THESIS

Lucija Jurko

Parent number: 58

Split, October 2017.

UNIVERSITY OF SPLIT

FACULTY OF CHEMISTRY AND TECHNOLOGY

Graduate study of Chemistry

Orientation: Organic Chemistry and Biochemistry

SURFACTANT-FREE MICROEMULSIONS: POSSIBLE APPLICATIONS FOR SOLUBILISATION AND EXTRACTION OF HYDROPHOBIC COMPONENTS

DIPLOMA THESIS

Lucija Jurko

Parent number: 58

Split, October 2017.

SVEUČILIŠTE U SPLITU

KEMIJSKO-TEHNOLOŠKI FAKULTET

Diplomski studij Kemija

Smjer: Organska kemija i biokemija

MIKROEMULZIJE BEZ PRISUTNOSTI SURFAKTANTA: MOGUĆE PRIMJENE ZA OTAPANJE I EKSTRAKCIJU HIDROFOBNIH KOMPONENATA

DIPLOMSKI RAD

Lucija Jurko

Matični broj: 58

Split, listopad

Surfactant-free microemulsions: possible applications for solubilisation and extraction of hydrophobic components

Lucija Jurko, 58

Abstract: This work deals with surfactant-free microemulsions (SFME) and is composed of two parts. In the first part these kind of ternary systems were investigated as a possible alternative for toxic extraction solvents that are still in use. In the second part pre-structuring of hydrotropes in water was studied, and its influence on the solubilisation of a third, hydrophobic component. Solvent extraction is widely used as a separation method. With the evolution of green chemistry new solvents are required with properties such as low toxicity and easy separation. SFMEs are considered as possible alternatives due to their better wetting properties and their possibility of solubilisation of hydrophobic components. Such solubilisation properties depend on the formation of supramolecular aggregates that typically occur in such systems. Three systems were investigated for this purpose: oleic acid/solketal/H_2O, glycerol triacetate/EtOH/H_2O and triethyl citrate/EtOH/H_2O. All systems showed pronounced mesoscale structuring near the phase separation border proved by DLS measurements. Ternary system oleic acid/solketal/H_2O was a "proof of principle system" of a cleavable SFME suitable for green extraction. Recently, it was established that structuring of binary mixtures of short chain alcohols/H_2O have a significant influence on the solubilisation of hydrophobic compounds such as benzyl alcohol and limonene. Second part of the work was focused on the study of more versatile hydrotropes such as dimethyl sulfoxide (DMSO), dimethylformamide (DMF), acetonitrile (ACN), dioxane, ethanol (EtOH), *tert*-butyl alcohol (TBA), γ-valerolactone (GVL) and tetrahydrofuran (THF). DLS and conductivity measurements were carried out to demonstrate the presence of structures in the binary and ternary mixtures.

Keywords: surfactant-free microemulsion, solubility, extraction, solketal, limonene, benzyl alcohol

Thesis contains: 75 pages, 18 figures, 1 table, 8 supplements, 91 references

Original in: English

Defence committee: 1. Ani Radonić - PhD, associate prof. - chair person
                  2. Senka Gudić - PhD, full prof. - member
                  3. Vesna Sokol - PhD, associate prof. - supervisor

Defence date: 27 October 2017.

Printed and electronic (pdf format) version of thesis is deposed in Library of Faculty of Chemistry and Technology Split, Ruđera Boškovića 35.

Mikroemulzije bez prisutnosti surfaktanta: moguće primjene za otapanje i ekstrakciju hidrofobnih komponenata

Lucija Jurko, 58

Sažetak: Ovaj rad se bavi mikroemulzijama bez prisutnosti surfaktanata te se sastoji se od 2 dijela. U prvom dijelu, ove vrste ternarnih sustava istraživane su kao zamjena za toksična ekstrakcijska otapala koja su još u upotrebi. U drugom dijelu proučavana je strukturiranost hidrotropa u vodi u pre-Ouzo području i njen utjecaj na otapanje hidrofobne komponente. Ekstrakcija je često korištena metoda odvajanja. Sve veći razvoj zelene kemije utjecao je na potražnju novih otapala koja ispunjavaju svojstva kao što su niska toksičnost i laka separacija. Smatra se da se mikroemulzije bez prisutnosti surfaktanata mogu koristiti kao zamjena za komercijalno dostupna ekstrakcijska otapala zbog boljeg svojstva kvašenja i mogućnosti otapanja hidrofobnih komponenata. Takva svojstva otapanja uvelike ovise o stvaranju supramolekularnih agregata koji se u pravilu odvijaju u ovim sustavima. U ovom radu ispitivana su tri sustava: oleinska kiselina/solketal/H_2O, glicerol-triacetat/EtOH/H_2O i trietil-citrat/EtOH/H_2O. Svi sustavi pokazali su strukturiranost blizu granice faza, što je i dokazano DLS mjerenjima. Ternarni sustav oleinska kiselina/solketal/ H_2O najviše se istaknuo kao sustav bez prisutnosti surfaktanata prikladan za zelenu ekstrakciju. Nedavno je utvrđeno da strukturiranost binarnih sustava kratkolančanih alkohola/H_2O ima veliki utjecaj na otapanje hidrofobnih komponenti poput benzil alkohola i limonena. Drugi dio rada usredotočen je na istraživanje različitih hidrotropa poput dimetil sufoksida (DMSO), dimetilformamida (DMF), acetonitrila (ACN), dioksana, etanola (EtOH), *tert*-butil alkohola (TBA), γ-valerolaktona (GVL) i tetrahidrofurana (THF). DLS i konduktometrijska mjerenja provedena su da se dokaže prisutnost struktura u binarnim i ternarnim sustavima.

Acknowledgments

Aims of the work

- To investigate ternary systems oleic acid/solketal/H_2O, glycerol triacetate/EtOH/H_2O and triethyl citrate/EtOH/H_2O as potential replacements for toxic solvents currently used for extraction, following the footsteps of Folch extraction model
- To study the influence of pre-structuring of DMSO, DMF, GVL, TBA, dioxane, ACN, THF, EtOH/H_2O binary mixtures on solubilisation of limonene and benzyl alcohol
- Conductometric studies and DLS measurements will be carried out to investigate the existence of structuring in monophasic region
- NMR measurements will be carried out to see the composition of the system after the cleavage

Summary

This work deals with surfactant-free microemulsions (SFME) and is composed of two parts. In the first part these kind of ternary systems were investigated as a possible alternative for toxic extraction solvents that are still in use. In the second part pre-structuring of hydrotropes in water was studied, and its influence on the solubilisation of a third, hydrophobic component.

Solvent extraction is widely used as a separation method. With the evolution of green chemistry new solvents are required with properties such as low toxicity and easy separation. SFMEs are considered as possible alternatives due to their better wetting properties and their possibility of solubilisation of hydrophobic components. Such solubilisation properties depend on the formation of supramolecular aggregates that typically occur in such systems.

Three systems were investigated for this purpose: oleic acid/solketal/H_2O, glycerol triacetate/EtOH/H_2O and triethyl citrate/EtOH/H_2O. All systems showed pronounced mesoscale structuring near the phase separation border proved by DLS measurements. Ternary system oleic acid/solketal/H_2O was a "proof of principle system" of a cleavable SFME suitable for green extraction.

Recently, it was established that structuring of binary mixtures of short chain alcohols/H_2O have a significant influence on the solubilisation of hydrophobic compounds such as benzyl alcohol and limonene. Second part of the work was focused on the study of more versatile hydrotropes such as dimethyl sulfoxide (DMSO), dimethylformamide (DMF), acetonitrile (ACN), dioxane, ethanol (EtOH), *tert*-butyl alcohol (TBA), γ-valerolactone (GVL) and tetrahydrofuran (THF). DLS and conductivity measurements were carried out to demonstrate the presence of structures in the binary and ternary mixtures.

Sažetak

Ovaj rad se bavi mikroemulzijama bez prisutnosti surfaktanata te se sastoji se od 2 dijela. U prvom dijelu, ove vrste ternarnih sustava istraživane su kao zamjena za toksična ekstrakcijska otapala koja su još u upotrebi. U drugom dijelu proučavana je strukturiranost hidrotropa u vodi u pre-Ouzo području i njen utjecaj na otapanje hidrofobne komponente.

Ekstrakcija je često korištena metoda odvajanja. Sve veći razvoj zelene kemije utjecao je na potražnju novih otapala koja ispunjavaju svojstva kao što su niska toksičnost i laka separacija. Smatra se da se mikroemulzije bez prisutnosti surfaktanata mogu koristiti kao zamjena za komercijalno dostupna ekstrakcijska otapala zbog boljeg svojstva kvašenja i mogućnosti otapanja hidrofobnih komponenata. Takva svojstva otapanja uvelike ovise o stvaranju supramolekularnih agregata koji se u pravilu odvijaju u ovim sustavima.

U ovom radu ispitivana su tri sustava: oleinska kiselina/solketal/H_2O, glicerol-triacetat/EtOH/H_2O i trietil-citrat/EtOH/H_2O. Svi sustavi pokazali su strukturiranost blizu granice faza, što je i dokazano DLS mjerenjima. Ternarni sustav oleinska kiselina/solketal/ H_2O najviše se istaknuo kao sustav bez prisutnosti surfaktanata prikladan za zelenu ekstrakciju.

Nedavno je utvrđeno da strukturiranost binarnih sustava kratkolančanih alkohola/H_2O ima veliki utjecaj na otapanje hidrofobnih komponenti poput benzil alkohola i limonena. Drugi dio rada usredotočen je na istraživanje različitih hidrotropa poput dimetil sufoksida (DMSO), dimetilformamida (DMF), acetonitrila (ACN), dioksana, etanola (EtOH), *tert*-butil alkohola (TBA), γ-valerolaktona (GVL) i tetrahidrofurana (THF). DLS i konduktometrijska mjerenja provedena su da se dokaže prisutnost struktura u binarnim i ternarnim sustavima.

Ključne riječi: mikroemulzije bez prisutnosti surfaktanta, topljivost, ekstrakcija, solketal, limonen, benzil alkohol

TABLE OF CONTENTS

LIST OFABBREVIATIONS

ACN	acetonitrile
cmc	critical micelle concentration
DMSO	dimethyl sulfoxide
DLS	dynamic light scattering
DMF	N,N-dimethyl formamide
EtOH	ethanol
h	hour
IPA	isopropyl alcohol (propan-2-ol)
NMR	nuclear magnetic resonance
NPA	*n*-propanol (propan-1-ol)
SANS	small-angle neutron scattering
SFME	surfactant free microemulsions
SWAXS	small-angle X-ray scattering
TBA	*tert*-butyl alcohol
THF	tetrahydrofuran
GVL	γ-valerolactone
wt %	weight percent

INTRODUCTION

Extraction is a separation method widely used in industry and in laboratory. However, adequate solvents are often hard to find, regarding basic principles of green chemistry [1, 2].

This relatively new branch of chemistry is concentrated on non-toxic, reusable systems. Numerous publications are dealing with this subject, trying to incorporate less hazardous chemicals in order to minimize the formation of pollutants. Green chemistry has a wide spectrum where it can be included [3].

Following the Folch extraction method, surfactant-free microemulsions (SFMEs) are used as potential solvents for extraction. One of the properties, which inspired their investigation for this purpose, was the so-called pre-Ouzo effect. It was found that structuring, usually found in the pre-Ouzo region, in some cases, promotes solubilisation. With changing the amount of just one component, easy separation of the oil and water rich phases is possible, to some extent [1, 2].

In this work, one of the main focuses is the investigation of the ternary system oleic acid/H_2O/solketal as a possible extraction solvent. The structuring of the system and cleavage of the used hydrotrope (solketal) was investigated. Furthermore, other systems such as glycerol triacetate, triethyl citrate/water/EtOH were introduced with cleavable oil phase as a separation method. In other words, two different methods were investigated in order to isolate the relatively pure oil and water phase, respectively (i) the usage of an easily cleavable hydrotrope (solketal) and (ii) the usage of a cleavable oil (glycerol triacetate/triethyl citrate). In both cases, the ternary system becomes more hydrophilic upon hydrolysis of one of the components and thus phase separation is induced.

Second project is the extension of a study done by Buchecker *et al.,* [4] which explained the influence of mesoscopic structuring of binary mixtures on the solubility of a third, hydrophobic component. In this study, it was found that pre-structuring of hydrotropes can be beneficial or obstructive for a good solubilisation of a hydrophobic component, depending on the chemical structure of this third hydrophobic compound. For benzyl alcohol it was found that pre-structuring is not favourable for a good solubilisation, whereas for limonene it is the other way round. This result was attributed to the fact that benzyl alcohol is able to induce mesoscale structures in ternary mixtures contrary to limonene, which can only intercalate in given pre-structures. Thus solubility of benzyl

alcohol and limonene in binary mixtures of short-chain hydrotropes/H_2O were investigated [4].

Goal of this part of the thesis is the investigation and a generalization of the concepts presented by Buchecker *et al.* for different hydrotropes such as DMSO, DMF, GVL, TBA, dioxane, ACN, THF and EtOH.

1. FUNDAMENTALS

1.1. Microemulsions

1.1.1. Definition and properties of classical microemulsions

Microemulsions were first discovered by Hoar and Schulman [5] in 1943 describing an optically transparent dispersion of water in oil. It was noticed that water, oil, surfactant (surface active component) and alcohol, form a homogeneous, transparent solution depending on their concentration. In their studies, hydrocarbons with long aliphatic chains were used as oil phase, and cetyltrimethylammonium bromide (hexadecyltrimethylammonium bromide) as surfactant.

According to IUPAC, microemulsions are thermodynamically stable and isotropic dispersions, formed by oil, water, surfactant and cosurfactant [6, 7, 8]. Although, these systems appear homogeneous, they often show the so-called Tyndall effect, which proves that microemulsions are heterogeneous on a microscopic level. Hoar and Schulman assumed that inverse micelles are formed in such systems, with surfactant molecules organized so that the polar side (hydrophilic "head") is turned to the center (water rich bulk phase) and the non-polar side (lipophilic "tale") orientated from the center to the outside (oil rich bulk phase) to reduce surface tension and thermodynamically stabilize the system. However, charged ends of surfactants repel each other. Thus, an alcohol (cosurfactant) is added to decrease the repulsion and to increase the flexibility of the interfacial film. Furthermore, the surfactant and cosurfactant molecules optimize the occupied area in the interfacial film in order to minimize the direct water/oil contact [9].

Spontaneous formation of aggregates will already occur in binary mixtures water/surfactant above a specific concentration of surfactant (critical micelle concentration - cmc). If the oil is dispersed in an aqueous pseudo-phase (oil-in-water (o/w) microemulsion), amphiphilic surfactant molecules will orientate with polar ends directing to the outer pseudo-phase (aqueous phase) and aliphatic chain towards the inner oil-rich pseudo-phase. For water-in-oil (w/o) microemulsions, it would be the other way. Winsor proposed different classification of microemulsions, dividing them into four types. Winsor type I has two phases in equilibrium: the bottom o/w microemulsion and an upper, almost pure oil phase (W_I in Fig 1). Winsor type II is composed of an upper w/o microemulsion and the bottom, almost pure aqueous phase

(W_{II} in Fig 1). Winsor type III has 3 phases; microemulsion (w/o, o/w or bicontinuous) in equilibrium with an upper oil phase and bottom aqueous phase (W_{III} in Fig. 1). Winsor type IV has one phase, clear and homogeneous microemulsion (W_{IV} in Fig. 1).

In Fig. 1, areas M1 and M2 represent compositions resulting in direct and reverse microemulsion systems. In area M1 only w/o microemulsions are present, in M2 inverse micelles or o/w microemulsions can be found [10].
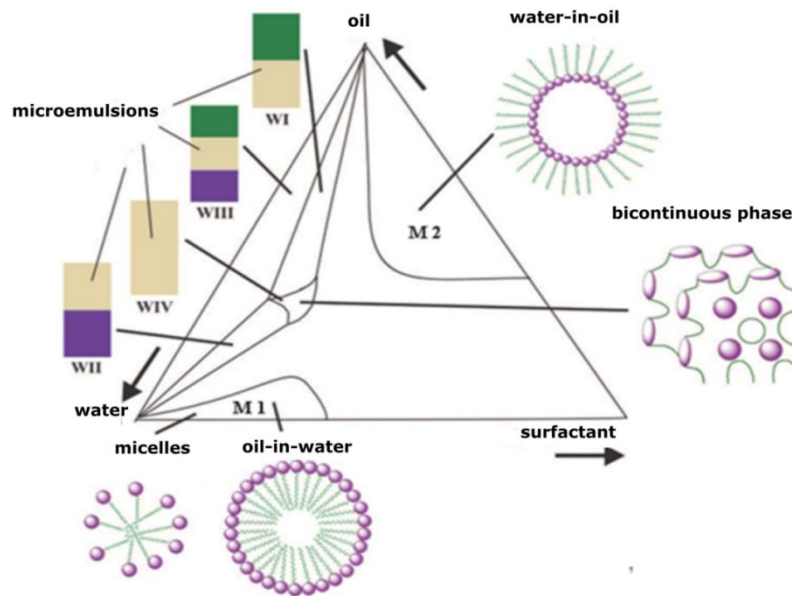
Figure 1. Ternary phase diagram for water/oil/surfactant ternary mixture with presented Winsor types. Redrawn from [6].

Because of their properties, microemulsions are widely used in different technologies; from food and textile industry, to production of detergents, in medicine, biomedicine and pharmacy (for controlled delivery of drugs) and in synthesis of nanoparticles [6, 7, 11].

1.1.2. Surfactants and hydrotropes

Surfactants or surface-active components are amphiphilic molecules with affinity to both, water and oil. That is possible due to their structure. They are composed of a hydrophilic "head", which is usually a very polar group or ion, and a hydrophobic "tail", usually a long aliphatic chain (C12 or higher). Above the cmc, surfactants adsorb at the interface and self-organize into larger supra-molecular structures. They tend to reduce the surface tension by creating a semi-fexible monolayer at the interface [1, 17, 18, 19]. Surfactants are mainly classified according to their hydrophilic group. Therefore, we distinguish anionic, cationic, non-ionic and amphoteric surfactants. Physio-chemical and microstructural properties dictate which type of surfactant should be chosen depending on the wanted application.

However, there is another type of organic compounds that facilitate the miscibility of water and oil, called hydrotropes [1, 10, 11]. Because of their shorter and/or branched aliphatic chain, they do not aggregate in ordered structures (compared to micellar systems) [16]. Furthermore, hydrotropes also form loose networks and highly fluctuating micelle-like clusters/aggregates [22]. By doing so, they can increase the solubility of a hydrophobic component.

Analogue to the CMC, the MHC- "minimum hydrotropic concentration" defines the minimum concentration of hydrotropes at which a structured homogenous solution can be expected to appear. However, the MHC is usually found to be much higher compared to the CMC [12]. One way it can be determined is by a change of slope of surface tension as a function of their concentration [21]. In addition, hydrotropes have a certain tendency to decrease the viscosity of surfactant solutions by breaking their ordered phases [27, 33].

Because of their countless characteristics, they already have applications in industry and great importance is attached to them in this work.

1.1.3. Surfactant-free microemulsions

1.1.3.1.   General information

Classical microemulsions are composed of oil, water and amphiphile (surfactant) [24], and for a long time, it was considered that a surfactant is necessary for the system to be stable. However, Smith and coworkers [25], while working with hexane/propan-2-ol/water ternary systems, realized that also SFMEs exist.

For classical microemulsion, above approximately 10 wt% of surfactant is needed to reach thermodynamic stability. This realization of Smith *et al.* led to conclusion that some systems do not need the surfactant to reach a stable monophasic and mesoscale structured region, which is economically more convenient, and expensive separation methods to separate surfactants from the product are avoided [2].

The SFME systems will be explained in more detail in later discussion.

1.1.3.2.   Ouzo effect

Ouzo effect, named after the Greek drink Ouzo, describes the formation of a highly stable emulsion. A hydrophobic component such as *trans*-anethole is dissolved in a water-miscible solvent (ethanol). Adding water in this binary mixture decreases the concentration of ethanol, spontaneously forming a milky emulsion. Pastis (France), Raki (Turkey), or Sambuca (Italy), which also contain *trans*-anethole, show the same effect with ethanol and water [26].

Even though this behavior was investigated in detail, some effects like narrow size distribution around 1 μm, and the kinetic stability of partly months could not be completely explained [1, 27].

This kind of emulsions has interesting properties, like monodispersity and remarkable time-stability without the presence of surfactants. It does not require energy for its formation; furthermore, stirring, change of pH value and ionic strength does not have significant effects, which make them the perfect fit for numerous industrial purposes [1, 27].

In medicine, the Ouzo effect is very helpful. Because these systems do not contain surfactants, the blood cell walls are not destroyed, so they can be used for intravenous purposes for drug delivery. Also, BASF company developed a procedure to make a water dispersible β-carotene used in food additives [28, 29, 89].

Two requirements have to be fulfilled for the Ouzo effect to appear [1, 30, 31, 32]. Regarding a three-component-system, component A has to be completely miscible with component B, but not soluble in component C, which is in turn completely miscible with component B. When component A is added rapidly in the binary mixture of components B and C, after crossing a certain concentration, oil/hydrotrope droplets are formed and the system becomes milky.

In the focus of this thesis is the pre-Ouzo effect which occurs right before the phase separation. Its properties will be described in the next chapter.

1.1.3.3. *Pre-Ouzo effect*

The pre-Ouzo effect occurs near the phase separation border when the requirements for Ouzo effect are fulfilled [19]. Previous studies of SFMEs deal with the investigation of mesoscale structures occurring in the so-called pre-Ouzo region. Observing for instance the ternary system water/ethanol/octan-1-ol with DLS and static light scattering, it was proven that well-defined domains exist in SFMEs [28, 31].

With increasing amount of water in the system, which means reaching the phase separation boundary, the correlation functions from DLS increase and get more pronounced. According to Klossek *et al.,* this is not a critical phenomenon because, some correlations can be found far from the demixing boundary. Static light scattering, neutron and X-ray scattering measurements further confirmed the existence of such nano-structures.

With increasing amount of EtOH, formed micellar-like aggregates swell. They have a defined size of a few nanometers and are in thermodynamic equilibrium. Further investigation of the solubilisation behavior with two hydrophobic dyes showed that SFME aggregates have a less hydrophobic core than classical microemulsion aggregates [28].

To get a better picture of structures of the octan-1-ol/ethanol/water system, Diat *et al.* combined small-angle neutron scattering (SANS) with wide- and small-angle X-ray scattering (SWAXS)[28, 37]. Schöttl *et al.* further investigated this effect using molecular dynamic simulations (see Fig. 3) [1, 34]. The results show that in this region, ethanol is distributed over both pseudo-phases. It causes the aggregates formed by octan-1-ol to swell, and reach about 2 nm in radius. At the interface EtOH is accumulated, and stabilizes the aggregates. This type of structuring gives these solutions microemulsion properties. They can be called surfactant-free microemulsions (SFME), because they fulfill the requirements of the IUPAC definition [1, 35, 91].

Klossek *et al.* tried to explain the formation of SFME. They developed a first model which comprises four terms shown in Table 1 [1, 36]:

Table 1: Terms influencing the formation of SFME and contribution to free energy taken from [1].

Van der Waals force	$dG(d) < 0$	Attractive dispersion forces between octanol-rich domains; Negligibly compared to other contributions
Mixing entropy of the dispersion	$dG(d) < 0$	Drives system towards smaller domains, favors mixing of the phases
Hydration force	$dG(d) > 0$	Repulsive hydration force between hydrophilic surfaces
Bending energy	$dG(d) > 0$	Free energy of the interfacial film; Weaker than hydration force

When all the terms are summed up, a minimum of free energy is found in the range of 2 nm – the typical radius of pre-Ouzo aggregates (see Fig. 2) [1, 36, 37].
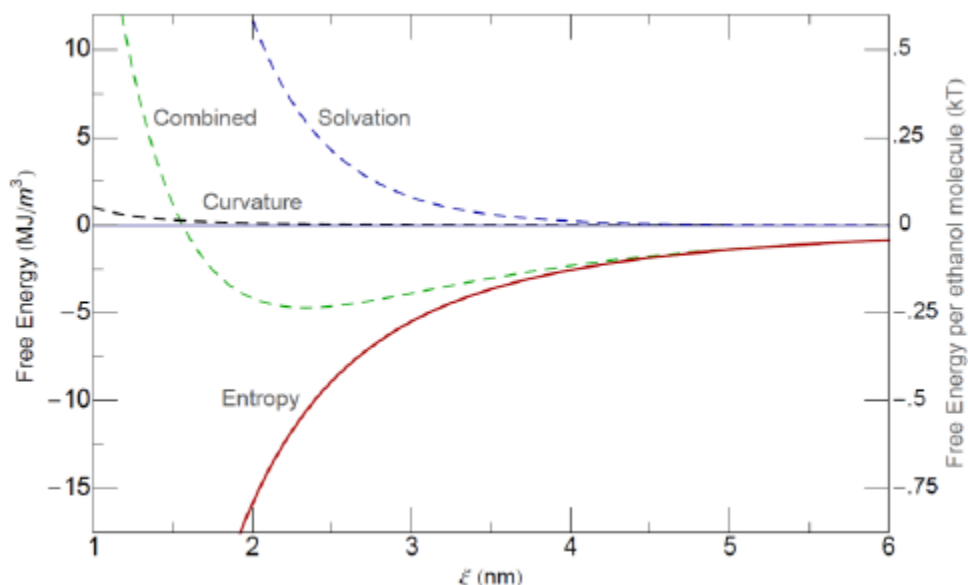
Figure 2. Total free energy per unit volume (left scale) and free energy per ethanol molecule (right scale) versus droplet radius [nm] showing the relative importance of the four contributions. Van der Waals forces are negligible and are not illustrated. The green curve shows the minimum of droplet size around 2 nm. Figure taken from [38].

Every system that fulfills the requirements for Ouzo effect, are not only characterized by an additional pre-Ouzo effect [18, 29]. Four characteristic domains were revealed with conductivity and surface tension measurements combined with DLS [1, 40, 41]. These domains are schematically represented in Fig. 3.

Only discrete aggregates are present in the ternary solution. But, bicontinuous phases can either be seen as coalesced reverse-micelle like aggregates or as coalesced sponge-like structured pre-Ouzo aggregates [1, 41].
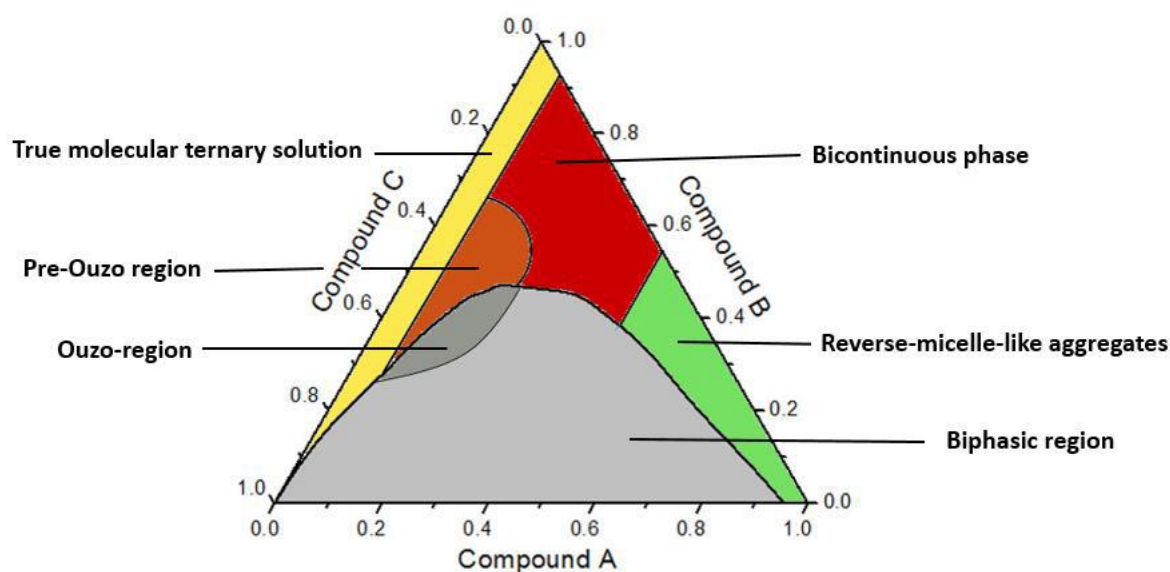
Figure 3. Schematic representation of characteristic domains present in surfactant-free microemulsions.

Properties of the pre-Ouzo region such as high contact surface, low interfacial tensions and good solubilisation were investigated to see if it can be applied for extraction [1].

1.1.4. Impact of pre-structuring of hydrotropes in water on the solubilisation of a hydrophobic compound

SFMEs are consisted of water, oil and hydrotrope. They have numerous applications and recently have been investigated in more detail. Structuring was found near the phase separation border, which was described in the previous chapter. As already mentioned, hydrotropes have an important role of stabilizing the aggregates, but also have the capability of solubilizing hydrophobic compounds in the hydrophilic solvent. SFMEs that show structuring, have hydrotropes accumulated at the interface between water rich and oil rich domain, however distributing over both pseudo-phases, which was proven with SANS and MD simulations [4, 19, 49].

For hydrophobic components to dissolve in a hydrophilic environment, the concentration of the hydrotrope should be above c (hydrotrope) > 0.2-0.5 mol/L. This can be compared to the classical microemulsions, where the cmc, for solubilisation to occur, is typically c (surfactant) > 10^{-2}-10^{-5} mol/L [4].

The solubilisation of the hydrophobic component often starts to increase tremendously in the concentration range of c (hydrotrope) > 1 mol/L. The distance between the molecules of hydrotrope decreases with the increase of its concentration. At one point, the cluster formation occurs, causing the hydrophobic component to dissolve [4, 42].

As mentioned before, amphiphilic character of hydrotropes is not strong to induce self-aggregation leading to defined aggregates in water with a well-defined shape [4, 42]. However, some hydrotropes like TBA were found to form clusters or loose aggregates already in binary mixtures with water, creating inhomogenities on a nanometer level [4, 43-46].

The group of Shimizu *et.al.*, tried to describe hydrotropic solubilisation, as a balance between solute-hydrotrope interaction and hydrotrope-hydrotrope interaction [4, 47-63]. There were some disagreements whether pre-structuring of the hydrotrope in H_2O reduces the solubility of solutes or not [4, 51, 52].

Therefore, numerous papers were published, focused on structures in binary mixtures of short-chain alcohols and H_2O [4, 43-58]. The common conclusion was that mesoscopic inhomogenities are formed due to hydration of non-polar aliphatic chains of alcohols, and a creation of hydrogen-bond network between alcohols and H_2O [4, 44]. Proof of this theory was found for *tert*-butanol/H_2O mixture which showed pronounced structuring [4, 58-67, 69, 70]. In addition it was found that in some cases, depending on the used hydrotrope and the hydrophobic component, pre-structuring can be both, pivotal or obstructive for a good solubilisation of the hydrophobic component.

1.1.4.1. Solubilisation of benzyl alcohol and limonene in binary mixtures of alcohol/H$_2$O

Buchecker *et al*. [4] investigated the presence of structuring in EtOH, propan-2-ol (IPA), propan-1-ol (NPA) and TBA/ H$_2$O binary mixtures [4]. The conclusions were backed up with DLS, SWAXS, SANS and conductivity measurements. TBA/H$_2$O and NPA/H$_2$O showed pronounced structuring depending on their composition, unlike EtOH/H$_2$O and IPA/H$_2$O which showed less pronounced structures (in the case of EtOH/H$_2$O even a molecular distribution is expected). Afterwards, the third, hydrophobic component was added.

It was proven that the structuring, induced by a third, hydrophobic component, is crucial for pronounced solubilisation power [4, 51, 52, 71]. The existence of a pre-structured binary mixture only impedes the solubilisation of (in this case) benzyl alcohol [4].

However, in the case of limonene, the situation was found to be different. The pre-structured binary system of alcohol/H$_2$O only enhanced the solubilisation power (of the hydrophobic component).

Two different solubilisation mechanisms were proposed:

- Pseudo-bulk solubilisation of hydrophobic components in aliphatic-rich region of pre-structured binary solvent.
- Solubilisation in the interfacial film of hydrophobic, but still amphiphilic component [4].

The type of the hydrophobic component dictates which hydrotrope is going to be used as a solvent. If the hydrophobic component to be dissolved does not have a polar functional group (as in the case for limonene), the pre-structured binary system enhances its solubilisation, due to an intercalation of limonene within given pre-structures.

Hydrophobic component with a polar functional group (for example, benzyl alcohol) are able to interact with the hydrotrope and to induce structures in the resulting SFME by its own, causing the pre-structured binary system to be obstructive for its solubilisation (as described by Shimizu et al.) [4, 51, 52, 71].

In order to extend this work and to generalize the above mentioned concept THF, GVL, dioxane, DMF, DMSO, ACN were investigated in this thesis regarding their impact on the solubilisation of limonene and benzyl alcohol.

1.1.5. Folch system and surfactant-free micellar extraction

Liquid-liquid extraction, describes partition of a third component between two immiscible solvents (for example, ether/H_2O), depending on its higher affinity to one of the used solvents. However, for lipid extraction and purification, chloroform-methanol-water system is used as a solvent. The extraction method was described for the first time by Folch as well as Bligh and Dyer [2].

Main ability of this system is partial miscibility of chloroform in water and water in chloroform. This ensures solubilisation of all lipids independently of their volume and polarity in the chloroform-phase, whereas hydrophilic components dissolve in the water-rich pseudo-phase. Usually, methanol is used to guarantee a homogeneous mixture and after extraction, phase separation is induced by the addition of water. The thus created two phases show excellent separation leading to almost pure chloroform and water/methanol phases, which facilitates the separation of the extracted compounds. Although this system displays excellent properties for it to be used for extraction, the toxicity of chloroform and methanol, especially chloroform, makes it inappropriate for large-scale application [2].

In order to improve this method, numerous researches were conducted. It is important to find a solvent that show same abilities, but does not contain hazardous components. Different systems were investigated such as hexane/IPA/H_2O and heptane/ethyl acetate/H_2O. They showed lower efficiency, and still have toxic components [2].

1.1.5.1.   Extraction using the pre-Ouzo to Ouzo effect

SFMEs, because of their good properties like high contact surface and good solubilisation, are considered as potential extraction solvents. Also, intense agitation is not needed for forming a homogeneous phase, and it is assumed for structuring in pre-Ouzo region to boost extraction efficiency [1, 72].

Mainly, the oil rich pseudo-phase of microemulsions serves both, as hydrophobic compound and as extraction solvent [1, 73]. Changing the temperature, the microemulsion switches from the monophasic region to biphasic region. The principle is shown in Fig. 4.
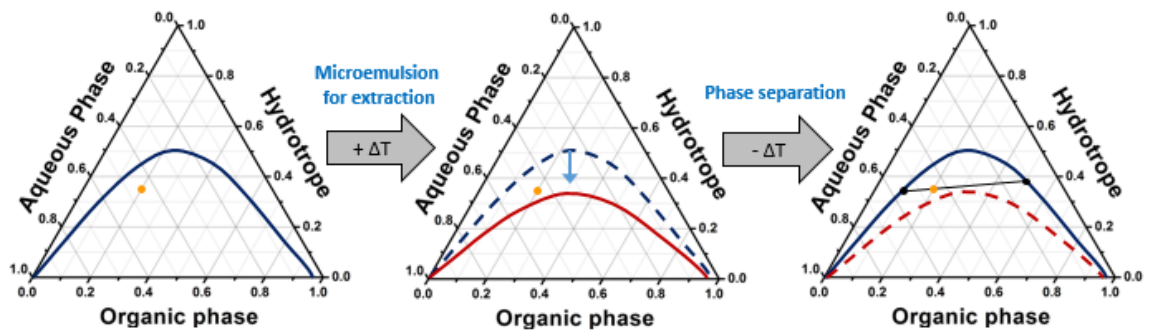
Figure 4. Main principle of Pre-Ouzo extraction. Figure taken from [14].

First, an emulsion is prepared with compositions of aqueous phase, oil phase and hydrotrope forming a biphasic mixture and the system is heated. According to the HLD concept, water becomes more hydrophobic due to weakening of hydrogen bonds [14]. Therefore, the biphasic region decreases and the chosen composition becomes a monophasic system. Now, extraction can be carried out. After the extraction is finished, the mixture is cooled, and the biphasic mixture is reformed consisting of an oil-rich and an aqueous phase separated according to the corresponding tie line. Distribution coefficient displays how the solutes are distributed between the two phases [71]. Consequently, phase separation can be induced by several approaches. For the Folch-method, the addition of water is used to cross the phase separation border. The concept presented above, on the other hand, uses a variation of temperature to control the transition from monophasic to biphasic and vice versa. Nevertheless, there are many other principles, which can be used to do so. In this work a new concept will be

presented using a chemical cleavage of one the components of the used microemulsion. This way, phase separation is induced in one of the two ways:

- cleaving the hydrotrope
- cleaving the oil phase

In both cases, the system gets more hydrophilic after the cleavage, which ensures a relatively proper phase separation.

CLEAVAGE OF THE HYDROTROPE

Solketal ((2,2-Dimethyl-1,3-dioxolan-4-yl)methanol) is an isopropyl ester of glycerol [77]. It is a stable molecule until it comes to contact with water, especially in acids or alkaline media, which catalyzes its hydrolysis into glycerol and acetone. This property is used for separation of the solute (apolar molecule) from the solvent (ternary system oleic acid/solketal/H_2O).

Adding water or acid in the ternary mixture, and accelerating the reaction by increasing the temperature, solketal separates into glycerol and acetone (Fig.5).
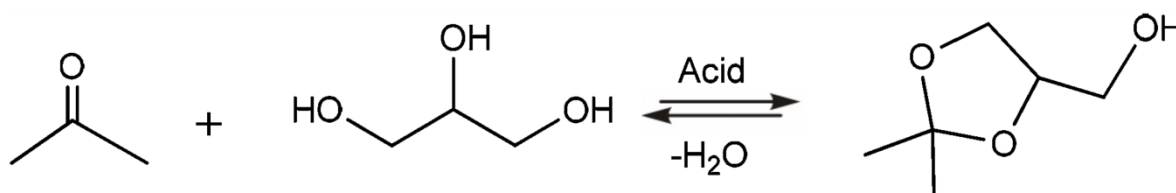
Figure 5. Condensation reaction of glycerol and acetone to obtain solketal [65].

Acetone, which is highly volatile, evaporates. H_2O and glycerol forms the lower phase and oleic acid forms the upper phase with the dissolved extracted component. The separation is now easy, but still the cleavage of the solute from the oleic acid needs to be investigated. Nevertheless, in this work, a proof of concept is presented, showing the principal suitability of such systems as solvents for extraction.

CLEAVAGE OF THE OIL PHASE

The cleavages of the ternary systems glycerol triacetate/EtOH/H_2O and triethyl citrate/EtOH/H_2O are based on the hydrolysis of the esters. Water and acid only induce their decompositions and high temperature accelerates the reactions. Glycerol triacetate separates into EtOH and acetic acid and triethyl citrate decomposes to EtOH and citric acid, with residues of ester (to be found).

In both cases monophasic and polar systems are formed, with extracted hydrophobic component creating a separate phase. The separation of such mixture is easy to achieve.

1.2.   Characterization of microemulsions

1.2.1.   Conductivity

There are three types of microemulsions: o/w microemulsions (oil droplets dispersed in aqueous medium); w/o microemulsions (water droplets dispersed in oil medium) and bicontinuous microemulsions. To determine the nano-structure and the film ridgidity of a microemulsion, conductivity measurement is an adequate method to use.

As already mentioned in the previous chapter, the interfacial film of microemulsions is very flexible. With increasing amount of water, conductivity curves of systems with this type of interfacial film show a typical bell-shape. The change of conductivity is shown on the system H_2O/SDS/1-pentanol/dodecane.

Percolation theory can explain this behavior [28, 76, 77-79]. The method for measuring the conductivity of the system is to add water into a w/o microemulsion. If it is needed, NaBr or other salt can be added to ensure the presence of enough charge carriers in order to obtain a measurable conductivity. For low water contents, the oil component is dominant, leading to low conductivity values, because there is not enough water for the charge exchange. With the increase of water, the conductivity rises till the percolation threshold Φ_p is reached. Below the threshold, water form aggregates in the oil phase. Adding more water to the mixture, the w/o aggregates are growing and getting closer to each other, and the transport of charge carriers can be carried out undistrubed. At Φp, the aggregates get too close and merge (percolation), forming a path (point T1 in Fig. 6) [28, 80, 81]. The curve deviates from linearity at higher water content, which indicates the formation of bicontinuous structures (points T2-T3) [28, 82, 83]. Maximum is reached, and rapidly decreases because of the formation of o/w microemulsion and dilution effects. For many systems, such as water/SDS/hexylamine/heptane, water/cetyltrimethylammonium bromide (CTAB)/n-pentanol/n-hexane conductivity measurements were preformed to understand these systems [28, 84, 85].
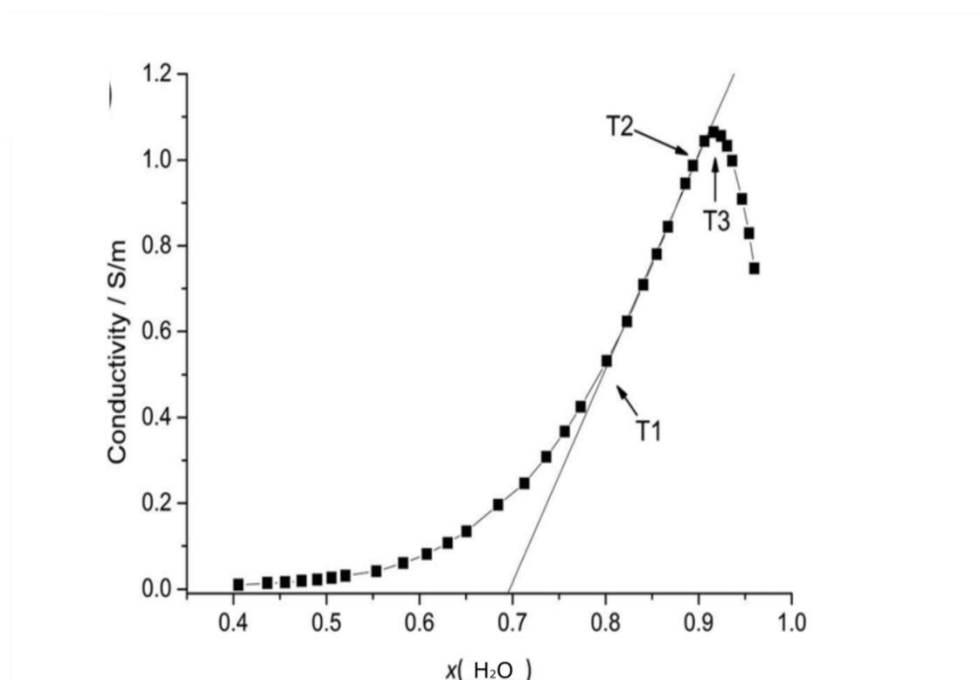
Figure 6. Conductivity curve for H_2O/SDS/1-pentanol/dodecane system. Figure taken from [4].

1.2.2. Dynamic light scattering (DLS)

Because of the difference in refractive indexes of colloidal particles, and the liquid in which they are dispersed, light will be scattered at the phase border between particles and the liquid. To get the information about the droplet/particle size and the corresponding diffusion coefficients, a time dependable analysis of fluctuations in the scattered light (DLS) is used.

Monochromatic light source with a wavelength λ (usually laser light) is used to illuminate the solution that is investigated by DLS. As explained above, if some colloidal particles exist; some of the light will be scattered in all directions. However, the diameter D of those particles has to be smaller than the wavelength of the monochromatic light; preferably D = λ/10 (Rayleigh scattering). Detector collect scattered light at a defined angle θ, and measure its intensity. The scattering vector q is defined as:

$$q \equiv k_S - k_I \qquad (1)$$

Where k_S is the propagation vector of the scattered light, and k_I is the propagation vector of the incident light (See Fig. 7) [28, 86].
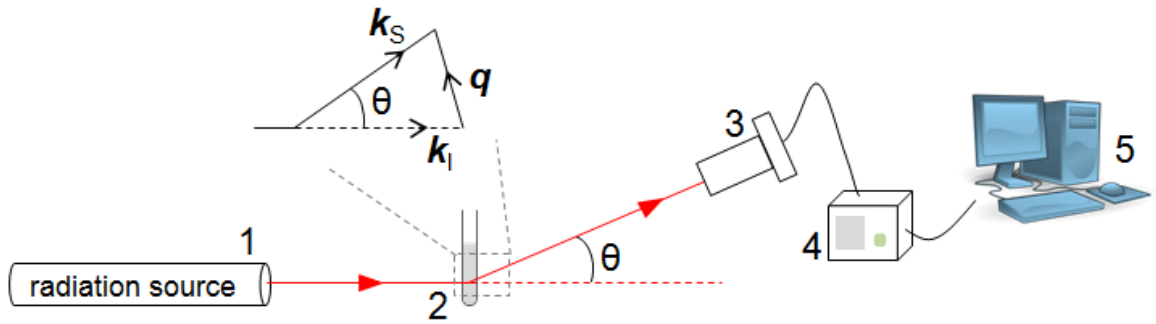
Figure 7. Representation of a DLS apparatus. The radiation source (1) delivers an incident light into the sample (2). The light is scattered and is collected by the detector (3) at a given angle θ. Light intensity data are fed to the correlator (4) that computes the correlation function of the intensity fluctuations. The correlation function is then displayed and analyzed on the computer (5). The scattering vector q is defined as the difference between the propagation vectors of the scattered and incident light, respectively k_S and k_I.

Since particles in solution undergo Brownian motion, the distance between them is constantly changing, and the medium is evolving. Measured intensity fluctuates over time because of the constructive and destructive interferences. The intensity fluctuations depend on the movement of the particles. The faster they move, the faster are the fluctuations. Smaller objects tend to give faster fluctuations and vice versa (Fig.8) [15, 18].
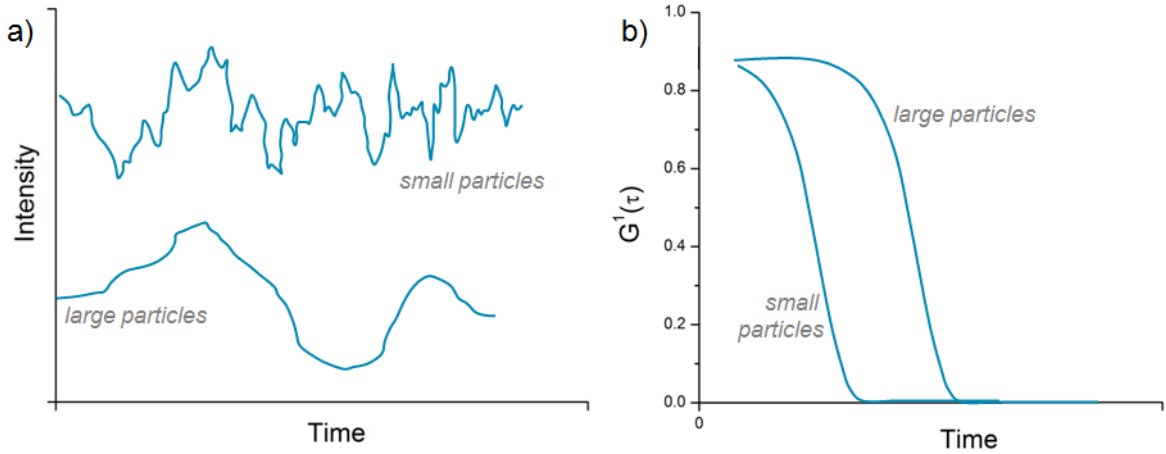
Figure 8. Illustrations of a) the intensity fluctuations; and b) correlation functions for small and large particles. Small particles are moving fast, so the signal is also changing fast and the correlation does not persist for a long time.

To compare the intensities of the signals at different time intervals, a digital autocorrelator is used. It measures how similar is a signal comparing to itself, but at a different time interval.

For example, comparing the intensities at time t and intensity a very small time later t + τ, a strong correlation is observed. Comparing successive intensity at a time t + 2τ to intensity at time t, the correlation is also present, but smaller. Following the pattern, the correlation will decrease until it is not detected anymore. Also, the size of the particles needs to be considered. As mentioned, larger particles move slower, so the change of the signal will be slower and the correlation will persist for longer time.

Time correlation function G1 (q,τ) at a particular scattering vector q can be calculated, as followed:

$$G_1(\boldsymbol{q}, \tau) = (I(\boldsymbol{q}, t) \cdot I(\boldsymbol{q}, t + \tau)) \qquad (2)$$

The time correlation function is a function of the correlator delay time τ, which decays exponentially. This applies for a large number of monodisperse objects both small and large, which undergo to Brownian motion. The following equation describes this function:

$$G_1(\boldsymbol{q}, \tau) = a_0 + (a_1 \times e^{-a_2 \tau})^2 \qquad (3)$$

a_0 is a constant base line value (usually 1), a_1 is dynamic part of the amplitude, and a_2 is the decay rate, used for the calculations of the diffusion coefficient thus for hydrodynamic radii (using Stokes-Einstein equation). For larger particles decay starts at a longer lag time, and other way round for smaller particles.

In this thesis, DLS is used as a technique for characterization of microemulsion droplets [15, 16].

2. EXPERIMENTAL

2.1. Chemicals

Ethanol (EtOH, purity $\geq$ 99.8%), (R)-(+)-limonene ($\geq$ 97%), *tert*-butanol (TBA, $\geq$ 99.7%), triethyl citrate ($\geq$ 98%), glycerol triacetate ($\geq$ 99%), oleic acid ($\geq$ 90%), *γ*-valerolactone (GVL, $\geq$ 98%), acetone ($\geq$ 99.5%) were purchased from Sigma-Aldrich (Steinheim, Germany). Acetonitrile (ACN, $\geq$ 99.5%), dioxane ($\geq$ 99.5%), N, N-dimethylformamide (DMF, $\geq$ 99.8%), sodium bromide ($\geq$ 99.99%), benzyl alcohol ($\geq$ 99%), sodium hydroxide (1 mol/L) were purchased from Merck (Darmstadt, Germany). Tetrahydrofuran (THF, $\geq$ 99.99%), dimethyl sulfoxide (DMSO, $\geq$ 99.99%) were purchased from Fischer Scientific (Loughborough, United Kingdom). Solketal ((2,2-dimethyl-1,3-dioxolan-4-yl)methanol) was purchased from Syntharo Fine Chemicals (Troisdorf, Germany). Hydrochloric acid (1 mol/L) was purchased from VMR Chemicals (Fontenay-sous-Bois, France) and dimethyl sulfoxide-d6 (99.5 atom% deuterated) from Deutero GmbH (Kastellaun, Germany).

2.2. Methods and Techniques

2.2.1. Ternary phase diagrams

Ternary phase diagrams were recorded using a static and dynamic process described by Clausse *et al.* [88]. In screw tubes, binary mixtures were prepared (3g), and the third component was added dropwise until a change in the phase behavior occurred. Phase diagrams were measured at 25°C and phase transition was observed with the naked eye. Weight and molar fractions were calculated from the mass of individual components obtained from precise weight measurements.

2.2.2. Dynamic light scattering

Before starting the measurement, the solutions were filtered using 0.2 μm PTFE membrane filters in order the remove dust and impurities. The samples were put into a temperature controlled toluene bath of a CGS-3 goniometer system from ALV (Langen, Germany) equipped with an ALV-7004/FAST Multiple Tau digital correlator and a vertical-polarised 22-mW HeNe laser (wavelength $\lambda = 632.8$ nm). Data were collected for 300 s at 25 °C and at an angle of 90°. Since aggregates formed in SFMEs usually do not have well defined shapes and are highly fluctuating no calculations of the hydrodynamic radii were made. The DLS spectra were evaluated qualitatively with regard to their correlation coefficient and their lag time. As a rule of thumb, it was assumed that a higher intercept of the correlation function for small lag times and larger lag times of the correlation function represent the more time-stable and more pronounced structuring in the solution.

2.2.3. Determination of the critical point

The critical point corresponds to the ternary formulation (located directly at the phase separation border); where both separated phases have equal volumes. For a rapid, however rough determination, homogenous solutions near the phase separation border were prepared (that showed best defined correlation functions in DLS), and the water/oil was added till reaching the phase separation border. The formulations were kept over night at 25°C until complete phase separation occurred. Volume ratios were determined with the naked eye using volume scaled glass tubes.

2.2.4. Conductivity measurements

Conductivity measurements were carried out in a thermostatted measurement cell (25 ± 0.2 °C) under permanent stirring using a low-frequency WTW inoLab Cond 730 conductivity meter connected with a WTW TetraCon 325 electrode (Weilheim, Germany). Samples were prepared (20 g) and were filled in the measurement cell and successfully diluted with pure water. To each sample 0.03 wt% of NaBr was added to ensure a sufficient amount of charge carriers. Addition of the salt did not noticeably affect the phase behavior nor the microstructure of the solutions.

2.2.5. ^{1}H-NMR measurements

Samples were prepared by adding 1-2 drops of the sample and 0.65 mL of DMSO-d6. The measurements were carried out on Bruker Avance 300 (300 MHz). The chemical shifts are reported in δ (ppm) relative to DMSO (2.5 ppm). Characterization of the signals: s = singlet, d = doublet, t = triplet, quint = quintet, m = multiplet, dd = double dublet. Integration is determined as relative number of atoms.

3. RESULTS AND DISCUSSION

3.1. Studies of cleavable surfactant-free microemulsions for green extraction

3.1.1. Objectives

The objective of this project was the investigation of cleavable SFMEs as new green solvent systems for extraction processes. Two concepts for the solvent processing and purification after the extraction were used: (i) the usage of a cleavable hydrotrope (solketal) and (ii) the usage of a cleavable oil-phase (glycerol triacetate/triethyl citrate). In both cases, phase separation is induced by cleaving the hydrotrope/oil, leading to relatively pure water- and oil-phases. However, the used SFME has to fulfill many requirements to be applicable as a green solvent. (i) The used components should be non-toxic, readily available and easy to recover after the extraction process. Second (ii), the used SFME should provide a high solubilisation power for hydrophobic compounds, which can be achieved using SFMEs that show good compartmentation between the water- and oil-rich pseudo-phases. (iii) The cleavage of the hydrotrope/oil and thus the phase separation should be easy to perform and to control, leading to products, which are preferably non-toxic and easy to remove.

To this purpose, three different SFME were investigated that (in principle) fulfill these tasks to the greatest extend:

- Oleic acid, solketal, H_2O (cleavable hydrotrope)
- Glycerol triacetate, EtOH, H_2O (cleavable oil phase)
- Triethyl citrate, EtOH, H_2O (cleavable oil phase)

In addition two ternary systems consisting of water, acetone/EtOH and oleic acid were used as reference systems.

3.1.2. Cleavable SFMEs

3.1.2.1. Phase behavior

Ternary phase diagrams for the system oleic acid/solketal/H$_2$O are shown in Fig 9.
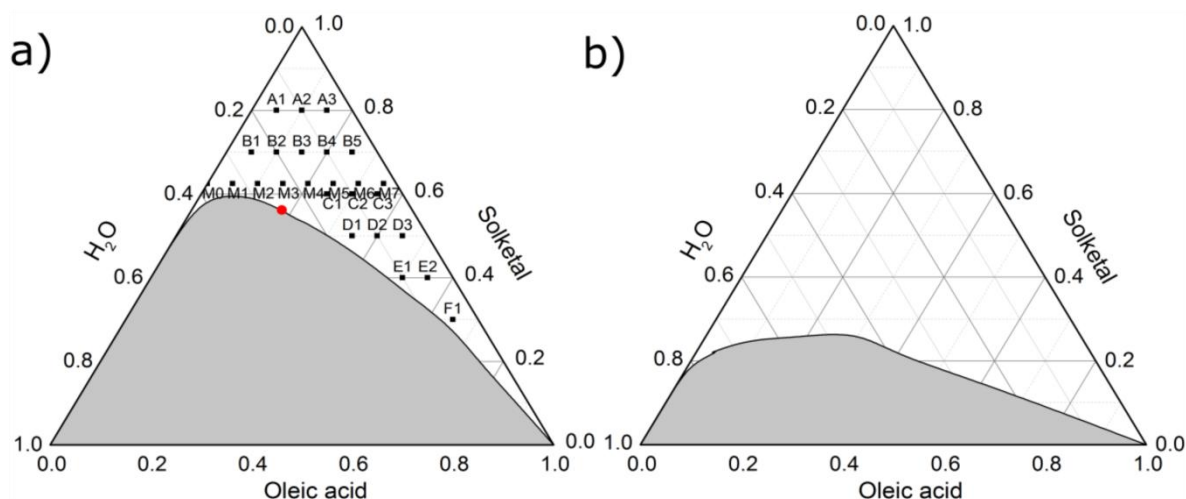
Figure 9. Ternary phase diagram of oleic acid/solketal/H$_2$O a) weight and in b) molar fractions. The grey area represents biphasic region, and the white area the monophasic region. Compositions investigated with DLS are denoted as black squares. The critical point is marked as red dot.

As expected, oleic acid and water show poor miscibility. Solketal on the other hand, was found to be completely miscible with water as well as with oleic acid. Thus, the basic requirements to form a SFME are fulfilled. The miscibility gap was found to be shifted to the water-rich region. Accordingly, a better solubility of water in binary mixtures composed of solketal/oleic acid was found than oleic acid in H$_2$O/solketal mixtures. For a solketal content of 60 wt%, full mixing of the three components is achieved, independent of the ratio of water/oleic acid.

To fully investigate possible SFME for the cleavage, H_2O, acetone/EtOH and oleic acid were used as reference systems. Phase diagrams given in weight fractions look similar to the one of the solketal.

To get more hydrophilic ternary mixture, the acetone is replaced with ethanol (Fig. 10 a). Using ethanol, the phase separation border is slightly lower compared to the one of solketal.
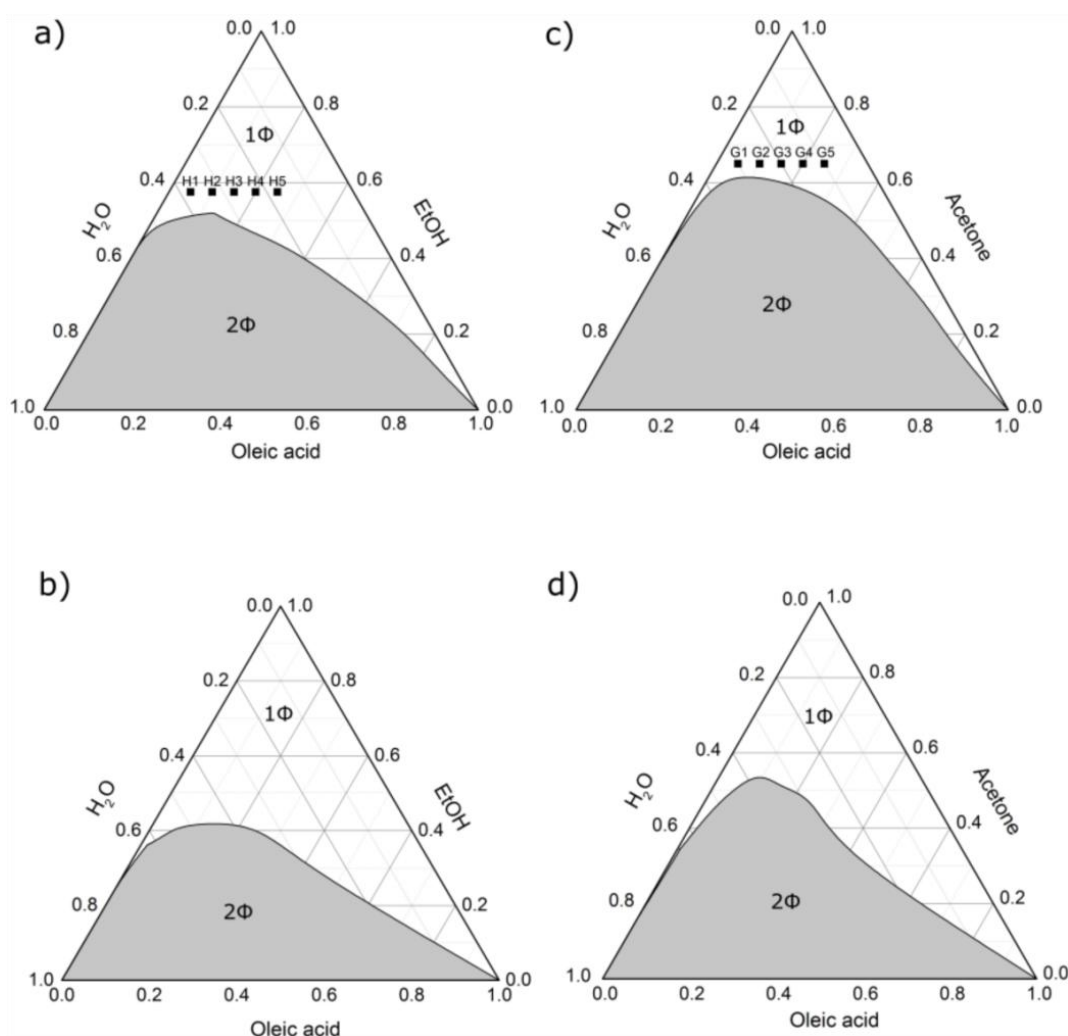
Figure 10. Ternary phase diagram oleic acid/EtOH/H_2O in a) weight and b) molar fractions and acetone /oleic acid/ H_2O in c) weight and d) molar fractions

Although, solketal shows comparable phase behavior regarding the phase diagram in weight fractions and DLS measurements (Fig. 9 and 12); seeing the phase diagrams in molar fractions, less acetone is needed for oleic acid/solketal/H_2O ternary mixture than for oleic acid/acetone/H_2O system to have the same characteristics.

Following the footsteps of Folch extraction model, system with easily cleavable hydrotrope was found. In that regard, ternary mixture oleic acid/solketal/H_2O showed good results. The second concept presented in this work is the usage of a cleavable oil component instead of a cleavable hydrotrope. To this purpose two hydrophobic esters, namely triethyl citrate and glycerol triacetate were tested in combination with H_2O and EtOH, used as a hydrotrope (see phase diagrams presented in Fig. 11).
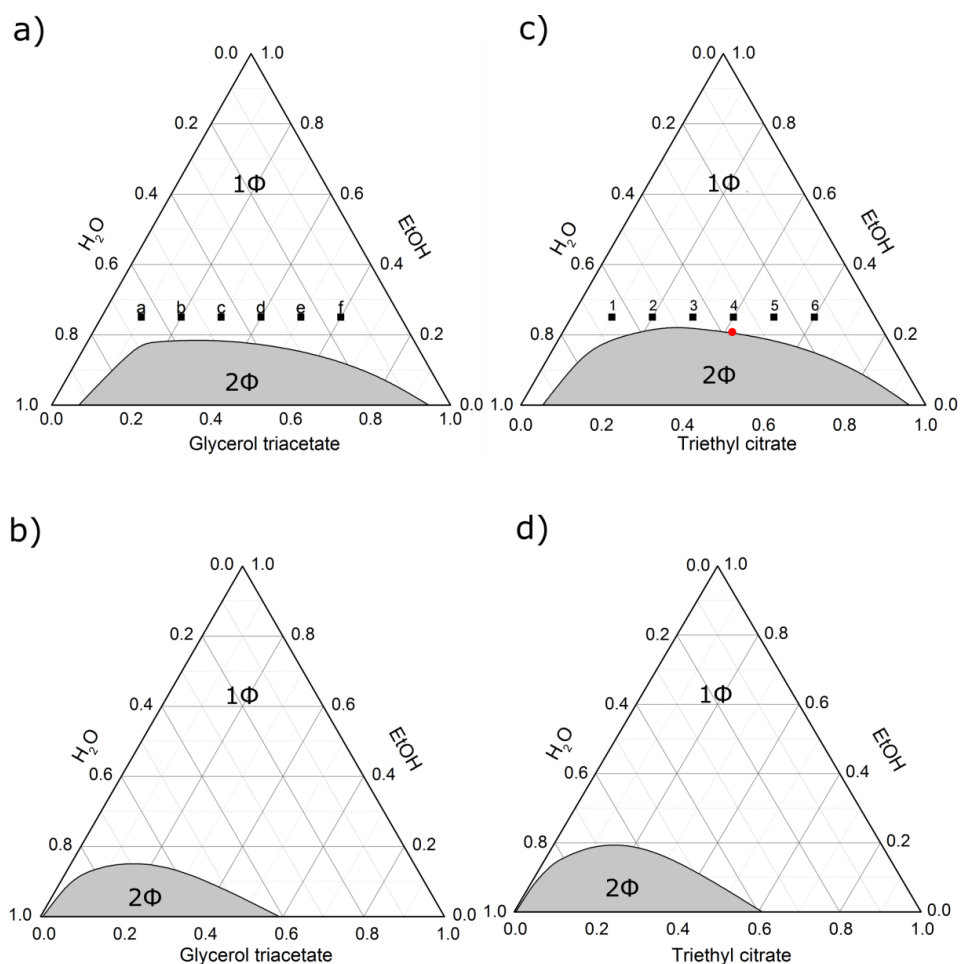
Figure 11. Ternary phase diagram glycerol triacetate/EtOH/H_2O in a) weight and b) molar fractions and triethyl citrate/EtOH/H_2O in c) weight and d) molar fractions. The critical point is marked as red dot.

Both systems show a similar phase behavior with a relatively low miscibility gap compared to the system oleic acid/solketal/H_2O.

However, in order to ensure a faster cleavage of the oil phase, glycerol triacetate should be used instead of triethyl citrate. Since EtOH is formed during cleavage of triethyl citrate, which is more volatile than the reaction products of the glycerol triacetate cleavage, faster reaction kinetics of the cleavage can be assumed in good approximation.

3.1.2.2.   Scattering experiments

In order to investigate possible mesoscale structuring present in the binary and ternary mixtures, DLS measurements were made for solketal/H_2O and oleic acid/solketal/H_2O mixtures (see Fig. 12).
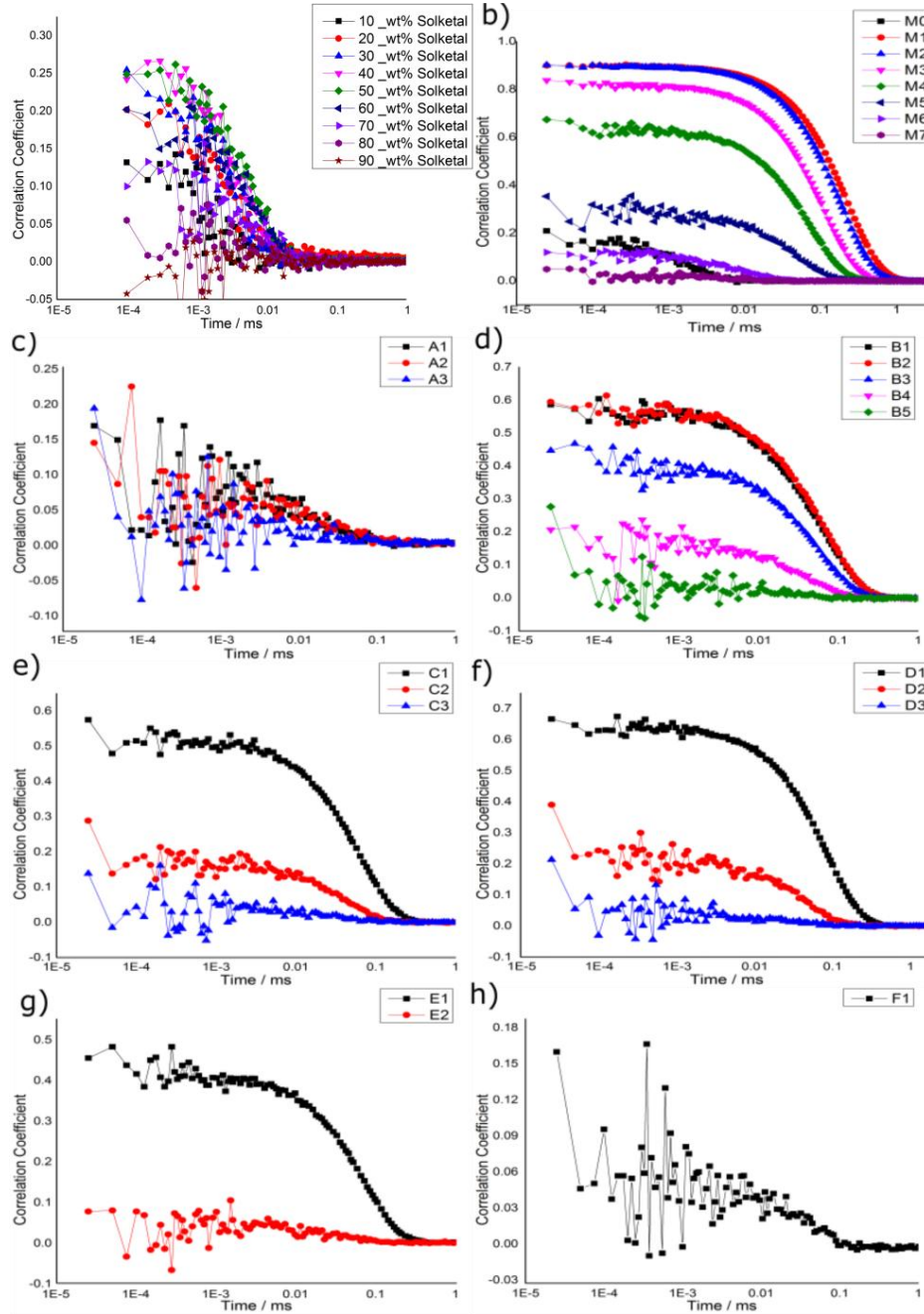
Figure 12. Self-correlation functions obtained by DLS measurements at 25 °C for the a) binary system of solketal / H_2O, b) ternary system of oleic acid/solketal/H_2O for points M0-7 c) points A1-3, d) points B1-5, e) points C1-3, f) points D1-3, g) points E1-2, h) point F1 (see also Fig. 9 a)

Regarding the results of DLS measurements for the binary mixtures solketal/H_2O (see Fig. 12 a), one can see pronounced correlation functions for almost any ratio of solketal/H_2O. Mixtures containing 40% and 50 wt% of solketal showed the best correlation. This indicates that already in the binary mixtures solketal/H_2O some sort of pre-structuring can be expected, leading to a compartmentation of solketal and water rich domains.

Upon addition of oleic acid, correlation functions get more and more pronounced, resulting in a shift to higher lag-times. This indicates strengthening and swelling of possible structures, which are already present in the binary mixtures. As expected, the best correlation function was found to be near the critical point (Figure 12 b-h). In addition, for high contents of solketal (80 wt%, points A1-A3) as well as for compositions near the binary axis of oleic acid/solketal, less defined correlation functions were obtained. Nevertheless, a large region could be detected (see Fig. 12 a), where significant mesoscale structuring can be expected, that indicates the presence of well-defined SFMEs leading to a compartmentation of aliphatic and water-rich domains on the nm-scale.

To see if these systems show a similar mesoscale structuring than the ternary system oleic acid/solketal/water, DLS measurements were performed. The samples were prepared close to the phase separation border (see Fig. 13).
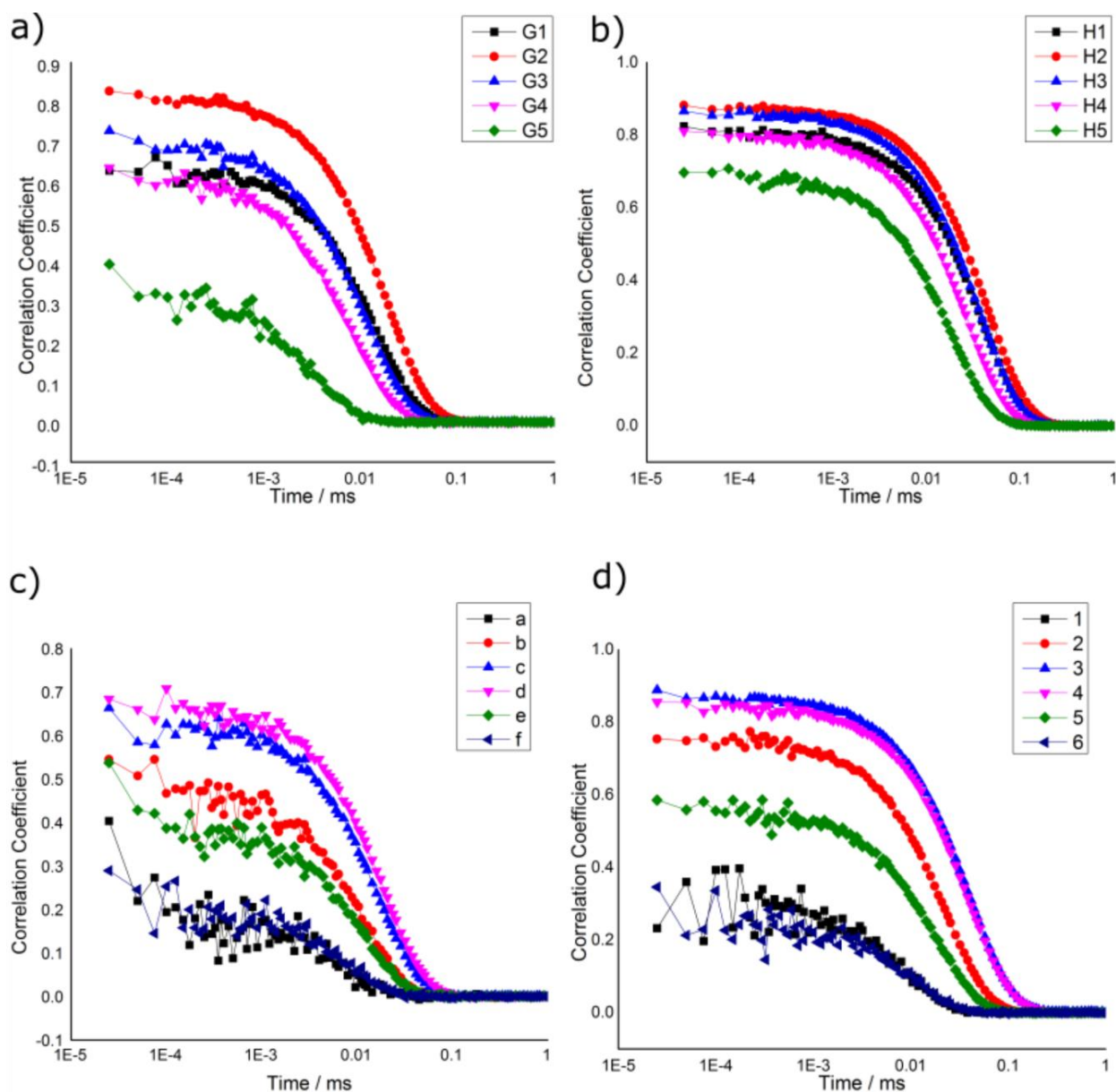
Figure 13. DLS measurement for ternary systems of a) oleic acid/EtOH/H$_2$O, b) oleic acid/acetone/H$_2$O, c) glycerol triacetate/EtOH/H$_2$O, d) triethyl citrate/EtOH/H$_2$O

For the oleic acid/EtOH/H_2O system, samples that are near the phase separation border (Fig. 13 a) show the best correlation. With increasing amount of the hydrophobic compound, the correlation decreases. As expected, structuring of the solution in the pre-ouzo region is observed.

Furthermore, the ternary system oleic acid/acetone/H_2O shows best correlation near the phase separation border (see Fig. 13 b), which means again that the most emphasized structures, can be observed in this region. Point H2 shows the highest correlation which is the closest to the biphasic region.

In conclusion, these two systems show similar behavior as the oleic acid/solketal/H_2O system.

The ternary mixture of glycerol triacetate, water and ethanol apparently shows mesoscale structured mixtures near the biphasic region as already found for other mixtures before. At point d, best correlation could be obtained (Fig. 13 c).

Triethyl citrate/EtOH/H_2O mixtures show similar correlations as those for glycerol triacetate. Most pronounced structuring is indicated at point 3 – nearest the miscibility gap and close to the critical point (Fig. 13 d).

EtOH and acetone show similar properties as solketal, but still do not show more stable or larger structures. The decay of their correlation functions are even at a smaller lag time.

Both esters have smaller biphasic regions, because of their structure. They form hydrogen bonds with EtOH and increase their solubility. Moreover, they show correlation functions near the miscibility gap which only adds to solubility.

According to the given results, the best properties show triethyl citrate/EtOH/H_2O system. Because of the formation of hydrogen bonds, it already has some strong binding in the pure system, and a large monophasic region to dissolve the desirable component.

3.1.2.3.   Titration

As already mentioned in section 1, the cleavage of solketal can be catalyzed using an acidic environment. Consequently, the kinetics of the solketal cleavage in aqueous solution should be strongly affected by the prevailing pH of the solution and can thus be controlled. In order to investigate this control of the solketal cleavage, titration experiments were performed (see Fig. 14).
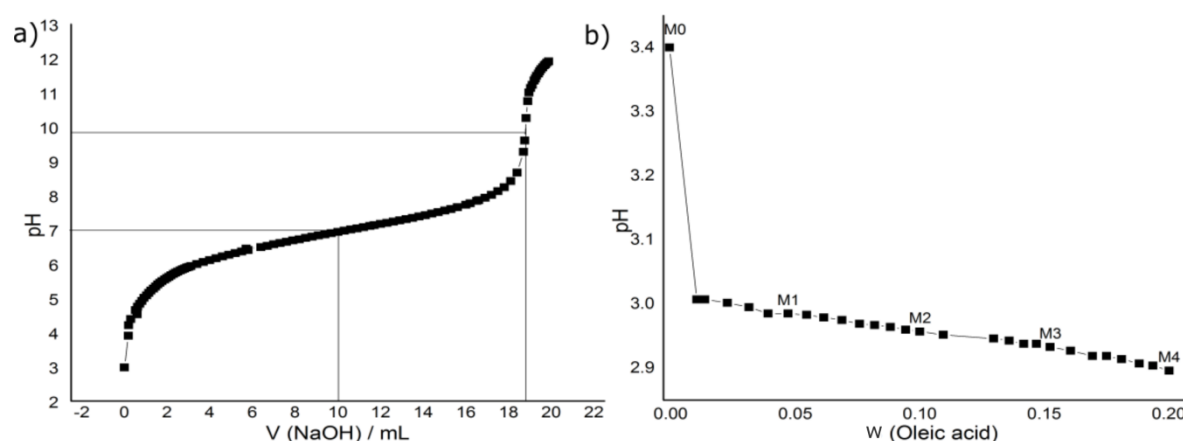
Figure 14. Titration curves of a) oleic acid/solketal/H_2O (point M2) with NaOH (*aq.* 1mol/L) and b) of solketal/H_2O (point M0) with oleic acid/solketal (0.375 weight fractions of oleic acid and 0.625 weight fractions of solketal)

Titration of composition M2 against NaOH showed that that pH is adjustable without phase separation of the whole mixture (Fig. 14 a). Therefore control of kinetics and the solketal cleavage is possible. pH 7 was reached with 10 mL of NaOH solution, and with the addition of 19 mL of NaOH solution, the equivalent point was attained.

It is already known that in more acidic environment the reaction is faster, but with the increase of the pH value, the kinetics is gradually getting slower. In this case, oleic acid reacts with NaOH and forms sodium oleate, which acts more like a surfactant. Consequently, the solution gradually becomes more and more like a classical microemulsion adding more and more NaOH, which prevents the solution from phase separation. Note that the same amount of water would cause the system to demix.

Nevertheless, adjustment of the pH and thus control of the solketal cleavage is feasible without demixing of the ternary mixture.

With the second titration the change of pH value with the addition of oleic acid/solketal to the binary mixture of solketal/H_2O was observed. This was done in order to investigate the influence of the amount of oleic acid on the solketal cleavage. To this purpose, the pH as a function of the amount of oleic acid is shown in Fig 14 b. After the first addition, there is a slight drop in the pH value from 3.4 to 3.0. Further addition of oleic acid does not significantly lower the pH anymore. Consequently, the amount of oleic acid in the SFME does only play minor role for the reaction kinetics of the solketal cleavage as the pH differences are small.

3.1.2.4.   *Cleavage of the hydrotrope*

To see if the system is suitable for extraction, it needs to be easily cleavable. Solketal cleavage could be successfully performed with 0.5 g oleic acid; 3.125 g solketal; 1.375 g H_2O (point M2 with an overall mass of 5 g) on a rotary evaporator at 60°C and 400 mbar for 6 hours.

An almost quantitative cleavage of solketal and removal of acetone was achieved with >98 % yield. The reaction was monitored using ^{1}H-NMR spectroscopy (see also supplementary material):

GLYCEROL
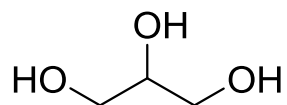
¹H-NMR (300 MHz, DMSO): δ_H = 3.32 (m, 5H), 4.51 (d, 1H), 4.431 (t, 2H)

OLEIC ACID
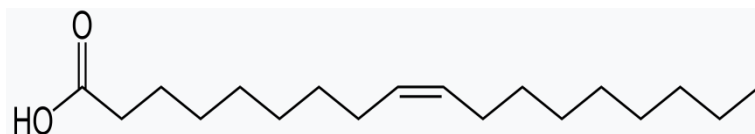
¹H-NMR (300 MHz, DMSO): δ_H = 0.85 (t, 3H), 1.23 (s, 18H), 1.47 (t, 2H), 1.98 (dd, 4H), 2.17 (t, 2H), 3.4 (s, 3H), 5.32 (t, 2H)

SOLKETAL
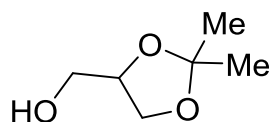
¹H-NMR (300 MHz, DMSO): δ_H = 1.25 (s, 3H), 1.30 (s, 3H), 3.395 (m, 4H), 3.63 (dd, 1H), 4.02 (t + quint, 2H), 4.82 (t, 1H)

PRODUCT AFTER SOLKETAL-CLEAVAGE – CRUDE MIXTURE (WATER + OIL PHASE)
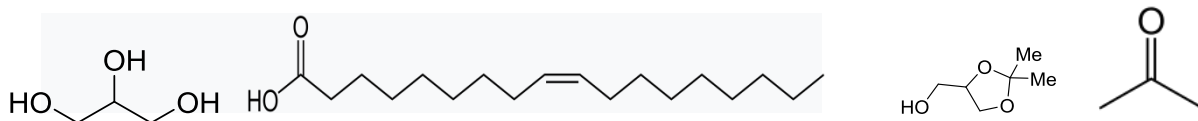
^{1}**H-NMR** (300 MHz, DMSO): δ_H = 0.848 (t, 3H), 1.23 (s, 18H), 1.46 (t, 2H), 1.97 (dd, 4H), 2.08 (s, 6H), 2.17 (t, 2H), 3.3 (m, 12H), 4.44 (s, 2H), 4.50(s, 1H), 5.32 (t, 2H)

PRODUCT AFTER SOLKETAL-CLEAVAGE - OIL PHASE
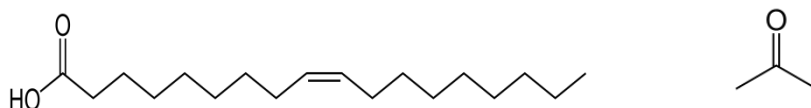
^{1}**H-NMR** (300 MHz, DMSO): δ_H = 0.85 (t, 3H), 1.23 (s, 18H), 1.47 (t, 2H), 1.98 (dd, 4H), 2.08 (s, 6H), 2.17 (t, 2H), 3.4 (s, 3H), 5.32 (t, 2H)

Looking at the spectrum of the crude mixture after the evaporation, one can observe peaks that correspond to the hydrogen atoms of glycerol (3.3, 4.4, 4.5 ppm); oleic acid (0.841, 1.24, 1.47, 1.97, 2.17, 3.3, 5.32 ppm), H_2O (3.4 ppm) and acetone (2.08 ppm). The conclusion that can be made from this is that solketal decomposes to glycerol and acetone completely; and after 6 h on 60 °C, only very small amounts of acetone remain in the mixture.

In addition, these measurements show that an almost pure oil phase can be obtained after cleavage of the hydrotrope. Consequently, a possible hydrophobic compound that is extracted can be isolated in an almost pure phase of oleic acid. Hydrophilic components on the other hand will be successfully separated in the resulting aqueous glycerol mixture.

The NMR spectra of pure solvents were recorded as a reference to exclude possible impurities of the starting materials and in order to facilitate the interpretation of the spectra.

3.1.2.5. Cleavage of the oil phase

Although the system glycerol triacetate/EtOH/H_2O showed similar behavior as triethyl citrate/EtOH/H_2O, their hydrolysis is different. The cleavage of glycerol triacetate, with the addition of acid, leads to its decomposition into to glycerol and acetic acid. From the less complex system a four component system is forming.

However, triethyl citrate hydrolyzes into ethanol, ester and citric acid, which also leads to formation of a more complex system.

In both cases with esters, if the same conditions are used for these systems as for the solketal (evaporator at 60°C and 400 mbar for 6 hours), a completely polar system is formed. If an apolar component is considered for extraction, it should precipitate or form a separate liquid phase and further separation is easy to achieve.

In conclusion, oleic acid/solketal/H_2O ternary mixture shows really good properties for extraction solvent. Structuring, in almost entire monophasic region, can be found, which increases its solubility power (if an apolar component is considered for extraction), and it is easily cleavable. In addition, it is found that less acetone is needed to get same phase behavior. For the cleavage of the oil phase, system glycerol triacetate/EtOH/H_2O showed better behavior, regarding reaction kinetics of the cleavage.

3.2. Influence of a mesoscale structuring of hydrotropes in water on the solubilisation of limonene and benzyl alcohol

3.2.1. Objectives

According to Buchecker *et al*. [4], prestructuring of hydrotropes in water can lead to better solubilisation of water immiscible components (e.g. limonene). Taking this idea into account, benzyl alcohol and limonene were investigated to see if they show similar solubilisation behavior with other possible co-solvents/hydrotropes. Phase diagrams, DLS, and conductivity measurements were made, all to determine if structuring in those ternary systems occurs and how it affects the solubilisation of the hydrophobic components.

Different hydrotropes such as: EtOH, TBA, DMF, dioxane, DMSO, GVL, THF, ACN were used for this purpose.

3.2.1.1. Phase diagrams

In order to find the compatibility of the benzyl alcohol and limonene with different hydrotropes and water, phase diagrams were recorded (see Fig. 15).
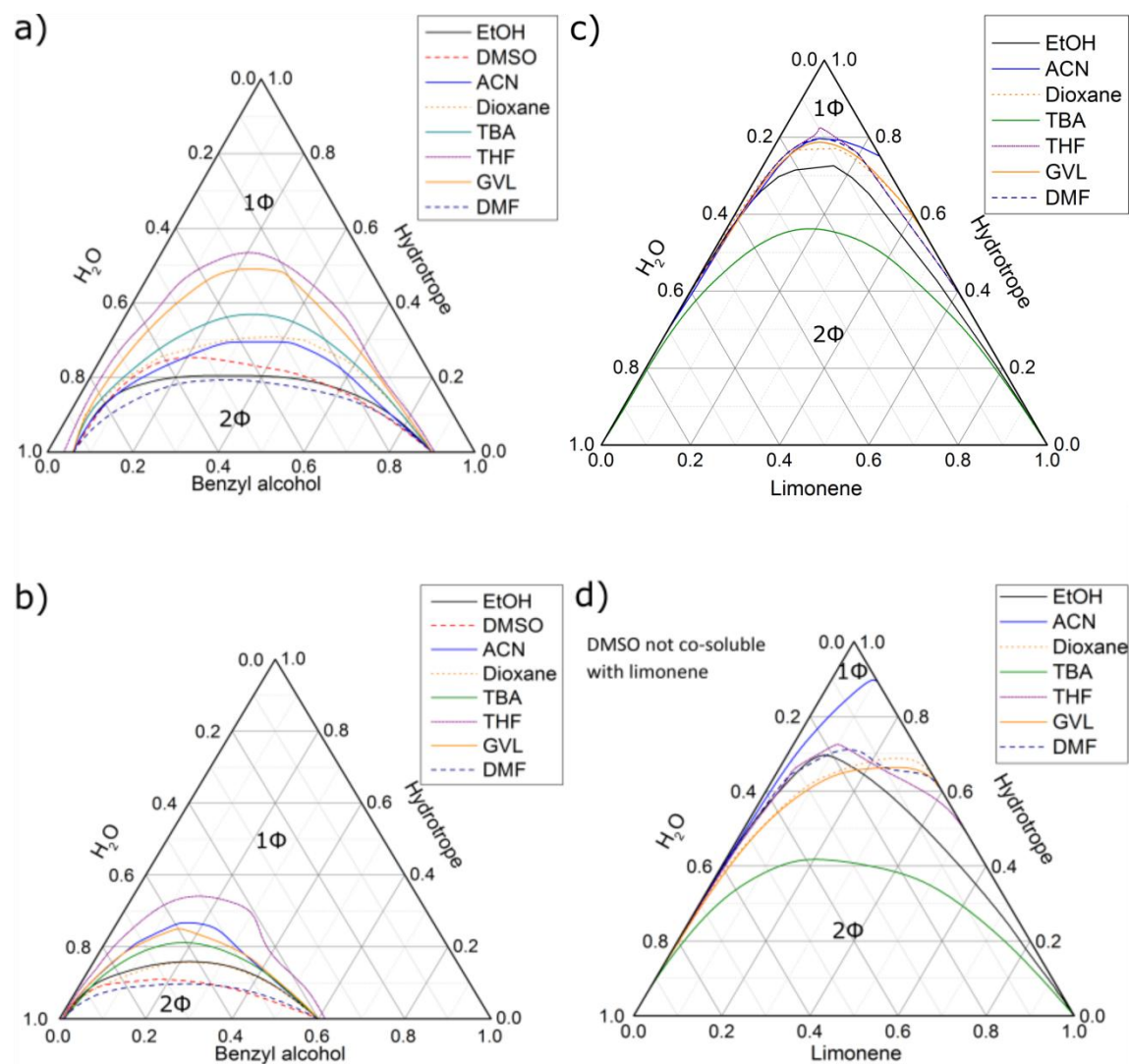
Figure 15. Ternary phase diagram benzyl alcohol/hydrotrope/water in a) weight and b) molar fractions and limonene/hydrotrope/water in c) weight and d) molar fractions. DMSO is not co-soluble with limonene.

The difference between limonene and benzyl alcohol is their miscibility with water. Benzyl alcohol is slightly miscible with water in comparison to limonene, which is poorly water miscible.

In case of benzyl alcohol, the solubilisation power of the hydrotropes decreases in the following order: DMF > EtOH > DMSO > ACN > dioxane > TBA > GVL > THF. It shows good compatibility with ethanol, DMF and DMSO but all the phase separation borders go less than 60 wt% of hydrotrope.

Seeing the phase diagrams (Fig. 15), one can see that limonene has higher miscibility gaps than benzyl alcohol. It is worth noting that limonene is not completely miscible with DMSO, so it was not possible to record the corresponding ternary phase diagram. The solubilisation power decreases in the following order: TBA > EtOH > dioxane > GVL >DMF ≈ ACN. Because of the poor miscibility with water, the phase separation border is higher than of benzyl alcohol, and it is in most of the cases closed at 80 wt % of hydrotrope.

3.2.1.2. DLS measurements

These ternary mixtures already fulfill the requirements to present the Ouzo effect; so points near the phase separation border were taken into consideration to see if they have structures in the pre-Ouzo region (see supplementary material). As well, to correlate possible mesoscale structuring of the systems with the solubilisation efficiency of the hydrotropes, DLS measurements were carried out.

BENZYL ALCOHOL

For comparison, DLS measurements for benzyl alcohol with the same hydrotropes were preformed. Correlation functions obtained by DLS measurements are shown in Fig. 16.
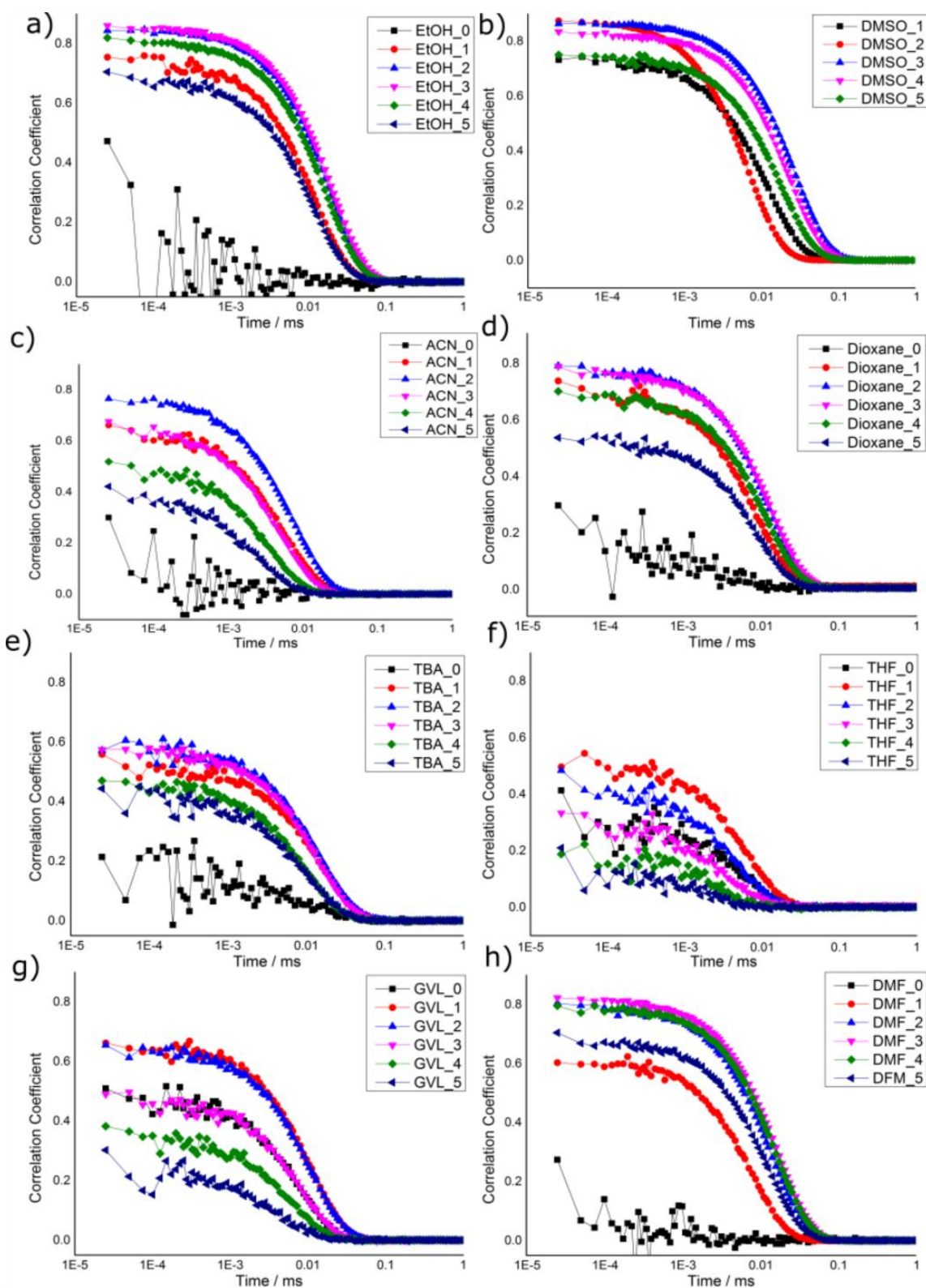
Figure 16. Self-correlation functions obtained by DLS measurements at 25 °C for the a) ternary system of benzyl alcohol/EtOH/H_2O, b) benzyl alcohol/dioxane/H_2O, c) benzyl alcohol/TBA/H_2O, d) benzyl alcohol/THF/H_2O, e) benzyl alcohol/GVL/H_2O, f) benzyl alcohol/DMF/H_2O

As already described by Buchecker *et. al.* [4], solubilisation of benzyl alcohol depends on pre-structuring of the binary mixtures.

There is no pronounced structuring found for binary mixtures of EtOH, DMF and ACN with water. With the addition of benzyl alcohol, the structuring was induced, because there are structures found for ternary mixtures.

Hydrotropes that show correlation for binary mixtures with water like DMSO, dioxane, TBA, THF and GVL lead to lower solubility of benzyl alcohol. Because of low miscibility with water, it dissolves in the oil-rich pseudo-phase, but also accumulates at the interfacial film due to the existence of alcohol polar group. This is supported by the fact that the ternary mixtures are less pronounced than the correlations for EtOH, DMF and ACN. In conclusion, pre-structured binary mixtures do not contribute to the solubilisation of benzyl alcohol; it only partially strengthens the structures.

LIMONENE
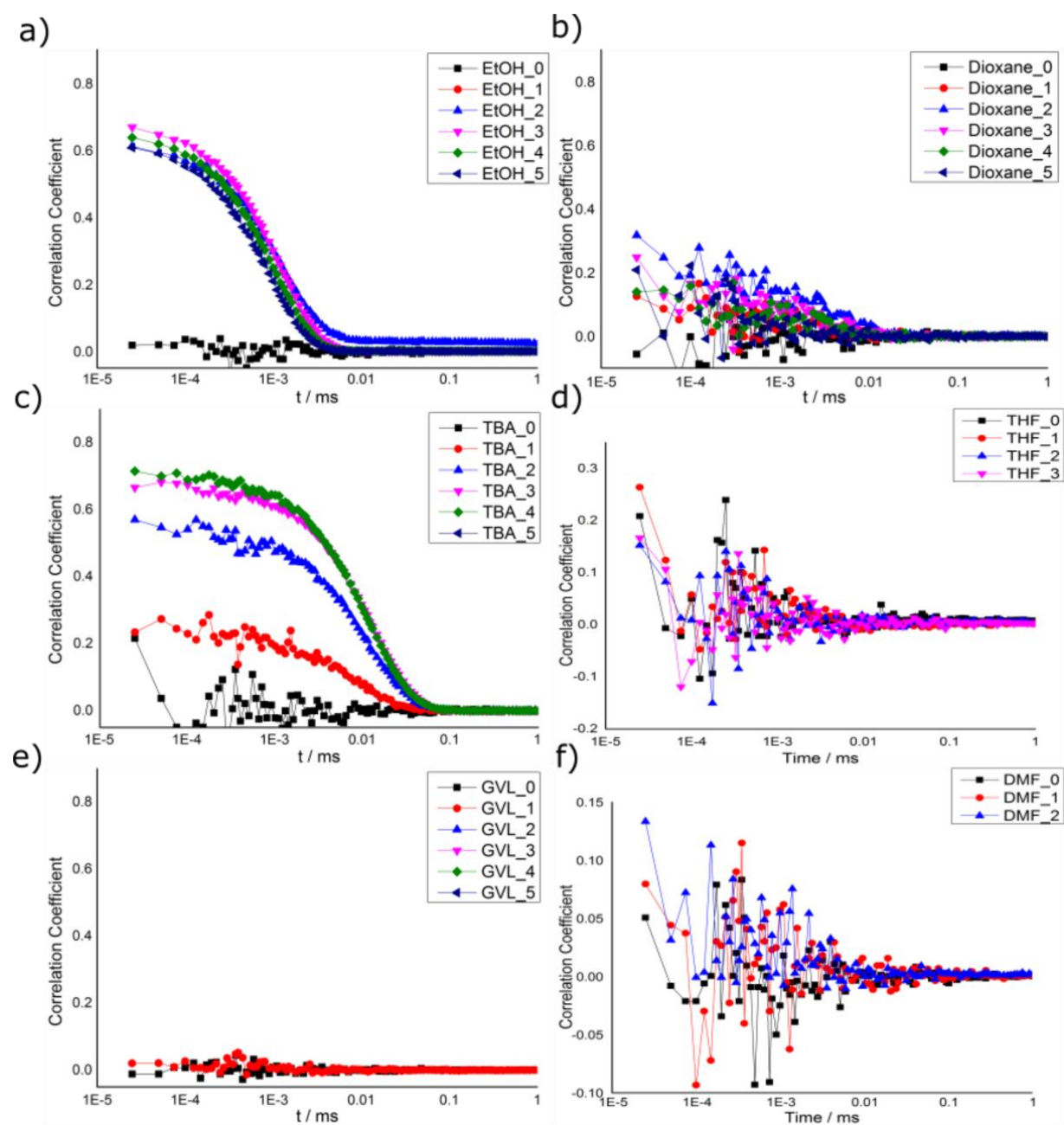
Figure 17. Self-correlation functions obtained by DLS measurements at 25 °C for the a) ternary system of limonene/EtOH/H_2O, b) limonene/dioxane/H_2O, c) limonene/TBA/H_2O, d) limonene/THF/H_2O, e) limonene/GVL/H_2O, f limonene/DMF/H_2O

Results obtained by DLS measurements indicate the presence of defined structured ternary solutions for TBA and EtOH. However, the decay of autocorrelation functions for TBA appears at a longer lag time. Larger fluctuating structures with lower diffusion coefficients give this kind of results. In these cases, limonene induces structuring because they were non-existent for binary mixtures with water.

Dioxane, THF, DMF, ACN,GVL, DMSO binary mixtures, did not show any correlations, but also there was no improvement after the addition of limonene; which leads to conclusion that limonene in these cases does not induce structuring.

3.2.1.3. *Conductivity measurements*

To further investigate structures of binary hydrotrope/H$_2$O and ternary benzyl alcohol/hydrotrope/ H$_2$O mixtures, conductivity measurements were performed.
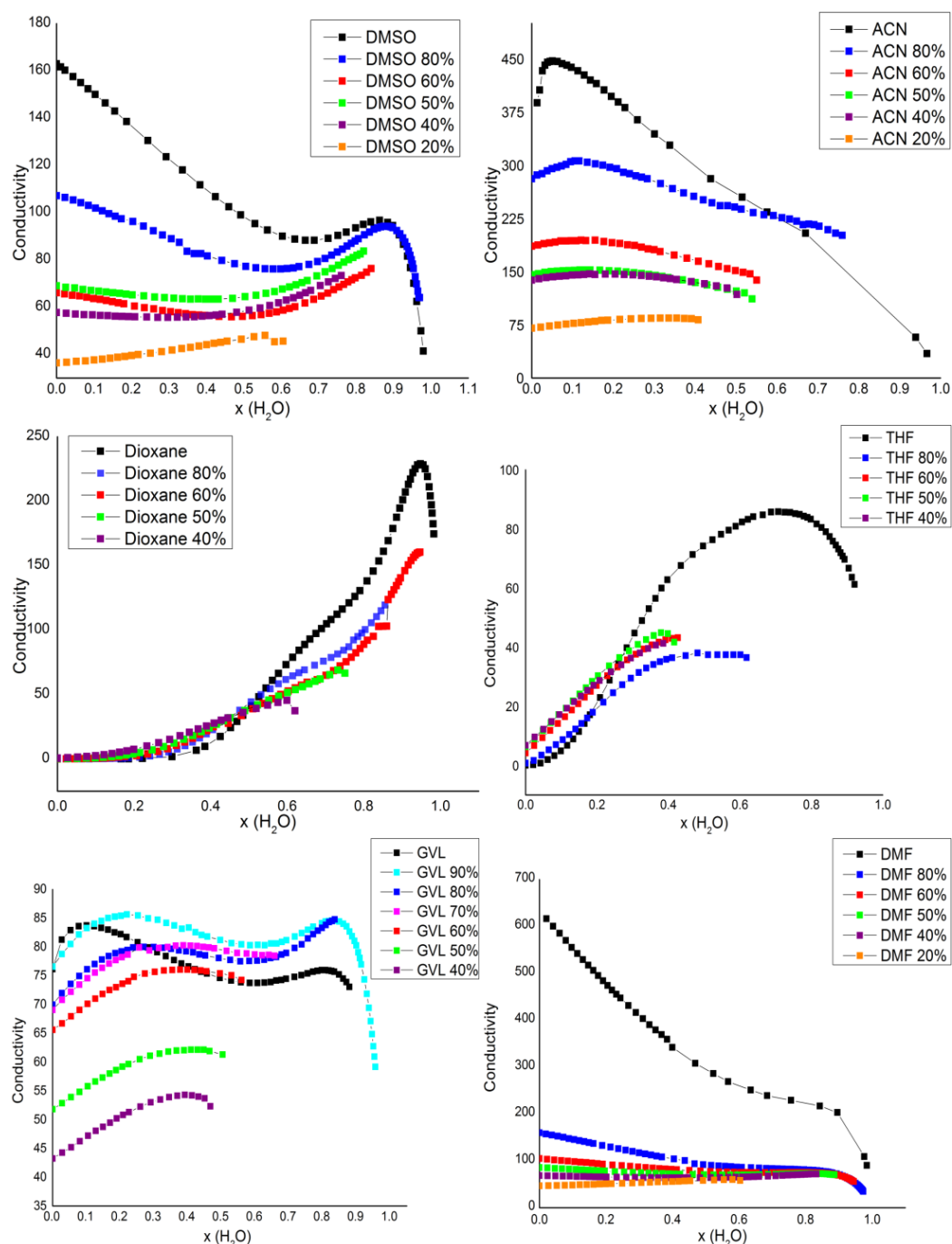
Figure 18. Conductivity measurements at 25 °C for binary and ternary mixtures of H$_2$O and benzyl alcohol with a) DMSO b) ACN c) dioxane d) THF e) GVL and f) DMF plotted in mole fractions of H$_2$O. To ensure measurable conductivities, 0.03 wt % of NaBr was added to the systems.

Conductivity measurements provide detailed information on the mobility of charge carriers and yield insight into the structuring of the systems [4, 66, 78, 79]. These measurements were made only for benzyl alcohol, because the biphasic regions are smaller than the ones with limonene.

For microemulsions that show structuring, change in conductivity is explained with the transition between w/o, bicontinuous and o/w microemulsions. With the increasing water content, the conductivity increases till the maximum. According to percolation theory, when we add water the micelle-like aggregates grow and merge, causing the formation of water channels, and the change of slope (increase of conductivity). It goes from a w/o microemulsion to an oil-rich bicontinuous microemulsion, and after the maximum, it shifts to water rich bicontinuous and later to o/w microemulsions.

Different concentrations of benzyl alcohol/hydrotrope binary mixtures were prepared, and to ensure enough charge carriers, in each solution 0.006 g of NaBr was added. For example, 80 wt% dioxane mixture contains 20 wt% of benzyl alcohol, 80 wt% of dioxane and 0.03 wt% of NaBr with a total mass of 20 g.

Since some of the hydrotropes used in this study, especially DMF, DMSO and ACN, have a relatively high permittivity of $\varepsilon > 35$ (at 25 °C), the conclusions derived from conductivity measurements at low water contents (x (water) < 0.5) are of low significance. In other words, the systems are hard to compare in this region and maxima observed (e.g. for ACN at x (H_2O) $= 0.05$) are likely to be just an effect of enhanced ion dissociation. Nevertheless, peaks/shoulders appearing at higher water contents (x (H_2O) > 0.5) can be often attributed to a change in solvent structure as described above. Consequently, measurements in this region can give useful hints on possible structures that might be formed. Furthermore the influence of benzyl alcohol on such structures can be investigated complementary to DLS measurements. Except of ACN containing solutions, all systems show a more or less pronounced peak/shoulder for high water content, which indicates again the presence of structured solutions and further supports the results obtained from DLS measurements. Furthermore, the influence of benzyl alcohol on the solvent structuring is not significant, as the shape of the curves does not change noticeably.

3.2.2. Discussion of the solubilisation mechanisms for limonene and benzyl alcohol

After conducting a series of various measurements, several mechanisms for solubilisation were proposed. The type depends on the existence of structuring in the system.

In principle, three pathways of the solubilisation are possible:

1. Solubilisation in the water-rich bulk phase,
2. Solubilisation in the oil-rich bulk phase
3. Solubilisation within the interfacial film

For EtOH, DMF, DMSO, and ACN weak or no correlation functions were found for binary mixtures with water. After the addition of benzyl alcohol, DLS measurements showed structuring, which led to conclusion that the hydrophobic component induces the formation of mesoscale structures. Because of these inhomogenities, the solubilisation of the oil component is enhanced and it is getting better with increasing amount of benzyl alcohol. It can be assumed that benzyl alcohol forms a hydrophobic core with benzyl alcohol also present to a certain amount at the interface (solubilisation mechanism 2 and 3). For limonene on the other hand, the missing pre-structuring of the binary mixtures leads to a lower solubility, since limonene is not able to induce structures by its own. In this case, a more molecular distributed solution is likely.

Dioxane, TBA, GVL and THF binary mixtures with water show measureable defined correlation functions. For structured systems like this, the solubilisation mechanism is different. The structuring, because it already exists without the oil component, is induced by the hydrotrope itself. Large areas of water-rich, oil-rich domains and interface are created. In this case, pre-structuring was found to be favorable to solubilize limonene, which can be intercalated in given pre-structures (solubilisation mechanism 2). This effect was found to be obstructive for a good solubilisation of benzyl alcohol. Within this study this finding could not be completely understood yet. Most plausible is that the resulting interfacial film is too rigid and that possible aggregates are difficult to form or get even destroyed.

Summing up, the choice of a suitable hydrotrope depends mainly on the chemical nature of the hydrophobic compound to be dissolved. In general it can be stated that a structure making hydrotrope should be used to dissolve a hydrophobic component, which is not able to induce mesoscale solvent structuring and vice versa.

4. CONCLUSION

- Main focus of this work was the investigation of aggregate formation in SFMEs regarding their interesting properties for e.g. high surface contact, good solubilisation properties and low interfacial tension.

- In the first part of this thesis, different cleavable SFMEs were introduced as possible extraction solvents. First time ever, a new concept for extraction solvent systems was presented: cleavable SFMEs using either a cleavable hydrotrope or, depending on its application a cleavable oil-rich pseudo-phase.

- Oleic acid/solketal/H_2O ternary system (representing a system with a cleavable hydrotrope) presented good results. The system revealed a relatively high miscibility within the ternary system oleic acid/solektal/H_2O, but after the investigation of the structuring, aggregates were found in almost entire monophasic region. This indicated very good solubilisation properties for dissolving hydrophobic component.

- Cleavage of the hydrotrope was induced with addition of H_2O and acid where higher temperature accelerated the reaction. This method was successfully carried out with reaching >98 % yield.

- In order to find a suitable SFME with cleavable oil phase, esters were investigated. Glycerol triacetate/EtOH/H_2O showed better results regarding faster reaction of the cleavage.

- Second part of the work dealt with solubilisation of hydrophobic components and the influence of mesoscale structuring on their solubilisation

- Solubility of limonene and benzyl alcohol in the binary mixures of EtOH, TBA, GVL, DMF, DMSO, ACN, dioxane and THF with H_2O were investigated Regarding benzyl alcohol; it was proven that pre-structuring of the binary mixtures only obstruct its solubilisation; while for limonene the pre-structuring only improve the solubilisation.

- Given results are in good accordance with the theory presented by Buchecker *et al.* and suggest an extension of the work presented therein.

REFERENCES

1. M. Pleines, *Extractant-free extraction using the pre-Ouzo to Ouzo effect*, *Diploma thesis*, Institute of Physical and Theoretical Chemistry, Regensburg, 2015.

2. C. Breil, M. Vian, T. Zemb, F. Chemat, *Int. J. Mol. Sci.,* 2017, **18**, 708.

3. https://en.wikipedia.org/wiki/Green_chemistry - 8.10.2017.

4. T. Buchecker, S. Krickl, R. Winkler, I. Grillo, P. Bauduin, D. Touraud, A. Pfitzner and W. Kunz, *Phys. Chem. Chem. Phys.*, 2017, **19**, 1806-1816.

5. T. P. Hoar, J. H. Schulman, *Nature*, 1943, **152**, 102-103.

6. B. K. Paul, S. P. Moulik, *Curr. Sci*., 2001, **80,** 990.

7. M. Malmsten, Microemulsion in Surfactants and Polymers in Drug Delivery. Marcel Dekker, New York, Basel, 2002.

8. J. Harrison, Speciality Chemicals Magazine, November 2004, 32–36. URL: www.specchemonline.com.

9. R. Zana, Dynamic Processes in Microemulsions, in R. Zana (ur.), Dynamics of Surfactant Self-Assemblies. Micelles, Microemulsions, Vesicles, and Lyotropic Phases. Taylor & Francis Group, Boca Raton, London, 2005, pp. 233–298.

10. P. A. Winsor, *Transactions of the Faraday Society,* 1948, **44**, 376–398.

11. M. J. Schwuger, K. Stickdorn, R. Schomäcker, *Chem. Rev*., 1995, **95,** 849.

12. P. Bauduin, F. Testard, T. Zemb, *The Journal of Physical Chemistry B,* 2008, **112**, 12354–12360.

13. B. A. Keiser, D. Varie, R. E. Barden, S. L. Holt, *J. Phys. Chem.,* 1979, **83**, 1276–1280.

14. G. Cravotto, L. Boffa, S. Mantegna, P. Perego, M. Avogadro, P. Cintas, *Ultrasonics sonochemistry,* 2008, **15**, 898–902.

15. A. M. Cazabat and D. Langevin, *J. Chem. Phys.*, 1981, **74**, 3148.

16. J. Rouch, A. Safouane, P. Tartaglia and S. H. Chen, *J. Chem. Phys.*, 1989, **90**, 3756.

17. D. F. Evans, H. Wennerström, *The colloidal domain. Where physics, chemistry and biology meet*, Wiley, New York, 1998.

18. C. Stubenrauch, *Microemulsions. Background, new concepts, applications, perspectives*, Wiley, Chichester, West Sussex, U.K., Ames, Iowa, 2009.

19. S. Schöttl, J. Marcus, O. Diat, D. Touraud, W. Kunz, T. Zemb and D. Horinek, *Chem. Sci.*, 2014, **5**, 2909-3340.

20. J. Eastoe, M. H. Hatzopoulos, P. J. Dowding, *Soft Matter*, 2011, **7**, 5917.

21. D. R. Karsa, *Industrial applications of surfactants IV.*

22. D. Subramanian, C. T. Boughter, J. B. Klauda, B. Hammouda, M. A. Anisimov, *Faraday Discuss*, 2014, **167**, 217.

23. P. Bauduin, F. Testard, T. Zemb, *The Journal of Physical Chemistry B*, 2008, **112**, 12354-12360.

24. I. Danielsson, B. Lindman, *Colloids Surf.*, 1981, **3**, 39.

25. G. Smith, C. E. Donelan, R. E. J. Barden, *Colloid Interface Sci.*, 1977, **60**, 488.

26. https://en.wikipedia.org/wiki/Ouzo_effect - 30.09.2017.

27. R. Botet, *J. Phys.: Conf. Ser.*, 2012, **352**, 012047.

28. J. Marcus, *Study of surfactant free microemulsions and microemulsions with fatty acid salts*, *Doctoral thesis,* Institute of Physical and Theoretical Chemistry, Regensburg, 2015.

29. J. Marcus, D. Touraud, S. Prevost, O. Diat, T. Zemb, *Influence of additives on the structure of surfactant-free microemulsions. Physical Chemistry Chemical Physics, Royal Society of Chemistry*, 2015, **17** (**48**), pp.32528-32538.

30. D. Horn, *Angew. Makromol. Chem.*, 1989, **166/167**, 139-153.

31. M. L. Klossek, D. Touraud, T. Zemb, W. Kunz, *Chemphyschem: a European journal of chemical physics and physical chemistry*, 2012, **13**, 4116-4119.

32. S. A. Vitale, J. L. Katz, *Langmuir*, 2003, **19**, 4105-4110.

33. J. Aubry, F. Ganachaud, J. P. Cohen Addad, B. Cabane, *Langmuir*, 2009, **25**, 1970-1979.

34. S. Schöttl, J. Marcus, O. Diat, D. Touraud, W. Kunz, T. Zemb and D. Horinek, *Chem. Sci.*, 2014, **5**, 2949.

35. V. Tchakalova, T. Zemb, D. Benczèdi, *Colloids and Surfaces A: Physicochemical and Engineering Aspects*, 2014, **460**, 414-421.

36. M. L. Klossek, D. Touraud, T. Lopian, J. Marcus, D. Horinek, S. F. Prevost, S. Schöttl, S. Marčelja, O. Diat, T. Zemb, W. Kunz, *PNAS*, 2016, **113**, 4260-4265.

37. O. Diat, M. L. Klossek, D. Touraud, B. Deme, I. Grillo, W. Kunz, T. Zemb, *J. Appl. Crystallogr*, 2013, **46**, 1665-1669.

38. T. N. Zemb, M. Klossek, T. Lopian, J. Marcus, S. Schöttl, D. Horinek, S. F. Prevost, D. Touraud, O. Diat, S. Marčelja, W. Kunz, *PNAS*, 2016, **113**, 4260-4265.

39. M. L. Klossek, D. Touraud, W. Kunz, *Phys. Chem. Chem. Phys.*, 2013, **15**, 10971-10977.

40. B. A. Keiser, D. Varie, R. E. Barden, S. L. Holt, *J. Phys. Chem.*, 1979, **83**,1276-1280.

41. P. Bošković, V. Sokol, T. Zemb, D. Touraud, W. Kunz, *The J. Phys. Chem. B*, 2015, **119**, 9933-9939.

42. P. Bauduin, A. Renoncourt, A. Kopf, D. Touraud, W. Kunz, *Langmuir: the ACS journal of surfaces and colloids*, 2005, **21**, 6769-6775.

43. D. Subramanian and M. Anisimov, *J. Phys. Chem. B*, 2011, **115**, 3179-9183.

44. D. Subramanian, C. T. Boughter, J. B. Klauda, B. Hammouda, M. Anisimov, *Faraday Discuss.*, 2013, **167**, 217-238.

45. M. Sèdlak, *J. Phys. Chem. B*, 2006, **110**, 13976-13984.

46. M. Sèdlak, D. Rak, *J. Phys. Chem. B,* 2014, **118**, 2726-2737.

47. S. Shimizu, N. Matubayasi, *J. Phys. Chem. B,* 2014, **118**, 10515-10524.

48. S. Shimizu, N. Matubayasi, *J. Phys. Chem. B,* 2014, **118**, 3922-3930.

49. S. Shimizu, N. Matubayasi, *Phys. Chem. Chem. Phys.,* 2016, **18**, 25621-25628.

50. T. W. J. Nicol, N. Matubayasi, S. Shimizu, *Phys. Chem. Chem. Phys.*, 2016, **18**, 15205-15217.

51. J. J. Booth, S. Abbott, S. Shimizu, *J. Phys. Chem. B*, 2012, **116**, 14915-14921.

52. J. J. Booth, M. Omar, S. Abbott, S. Shimizu, *Phys. Chem. Chem. Phys.*, 2015, **17**, 8028-8037.

53. S. Dixit, J. Crain, W. C. K. Poon, J. L. Finney, K. Soper, *Nature*, 2002, **416**, 829-832.

54. O. Gereben, L. Pusztai, *J. Phys. Chem. B*, 2015, **119**, 3070-3084.

55. A. Ghoufi, F. Artzner, P. Malfreyt, *J. Phys. Chem. B*, 2016, **120**, 793-802.

56. M. L. Tan, B. T. Miller, J. Te, J. R. Cendagota, B. R. Brooks, T. Ichiye, *J. Chem. Phys.*, 2015, **142**, 0645011.

57. L. Almasy, G. Jancso, L. Cser, *Appl. Phys,. A: Mater. Sci. Process.*, 2002, **74**, 1376-1378.

58. K. Nishikawa, H. Hayashi, T. Iijima, *J. Phys. Chem.*, 1989, **93**, 6559-6565.

59. D. T. Bowron, J. L. Finney, A. K. Soper, *J. Phys. Chem. B*, 1998, **102**, 3551-3563.

60. K. Yoshida, T. Yamaguchi, A. Kovalenko, F. Hirata, *J. Phys. Chem. B*, 2002, **106**, 5042-5049.

61. T. Fukasawa, Y. Tominaga, A. Wakisaka, *J. Phys. Chem. A,* 2004, **108**, 59-63.

62. A. A. Bakulin, M. S. Pshenichnikov, H. J. Bakker, C. Petersen, *J. Phys. Chem. A*, 2011, **115**, 1821-1829.

63. H. A. R. Gazi, R. Biswas, *J. Phys. Chem. A,* 2011, **115**, 2447-2455.

64. B. Kezic, A. Perera, *J. Chem. Phys.*, 2012, **137**, 0145011.

65. M. D. Hands, L. V. Slipchenko, *J. Phys. Chem. B,* 2012, **116**, 2775-2786.

66. L. Comez, M. Paolantoni, L. Lupi, P. Sassi, S. Corezzi, A. Morresi, D. Fioretto, *J. Phys. Chem. B*, 2014, **119**, 9236-9243.

67. D. Banik, A. Roy, N. Kundu, N. Sarkar, *J. Phys. Chem. B,* 2015, **119**, 9905-9919.

68. S. K. Allison, J. P. Fox, R. Hargreaves, S. P. Bates, *Phys. Rev. B: Condens. Matter Mater. Phys.*, 2005, **71**, 1-5.

69. P. G. Kusalik, A. P. Lyubartsev, D. L. Bergman, A. Laaksonen, *J. Phys. Chem. B,* 2000, **104**, 9526-9532.

70. M. Tomsic, A. Jamnik, G. Fritz-Popovski, O. Glatter, L. Vladek, *J. Phys. Chem. B,* 2007, **111**, 1738-1751.

71. W. Kunz, K. Holmberg, T. Zemb, *Curr. Opin. Colloid Interface Sci.*, 2016, **22**, 99-107.

72. R. Schott, A. Pfennig, *Molecular Physics*, 2006, **102**, 331-339.

73. T. Lopian, *Masterthesis*, Institute of Physical and Theoretical Chemistry, 2014, Regensburg.

74. V. Nardello, N. Chailloux, J. Poprawski, J. L. Salager, J. M. Aubry, *Polym. Int.*, 2003, **52**, 602-609.

75. Maria J. Climent, Avelino Corma and Sara Iborra*, Green Chem.*, 2014, **16**, 516-547

76. M. Clausse, J. Peyrelasse, J. Heil, C. Boned and B. Lagourette, *Nature*, 1981, **293**, 636-638.

77. B. Lagourette, J. Peyrelasse, J. Heil, C. Boned and M. Clausse, *Nature*, 1979, **281**, 60-62.

78. M. Lagues, R. Ober and C. Taupin, *J. Phys. Lett.*, 1978, **39**, 487-491

79. M. Lagues, *J. Phys. Lett.*, 1979, **40**, 331-333.

80. A. Ponton, T. K. Bose and G. Delbos, *J. Chem. Phys.*, 1991, **94**, 6879.

81. M. Lagues and C. Sauterey, *J. Phys. Chem.*, 1980, **84**, 3503-3508.

82. M. L. Klossek, J. Marcus, D. Touraud and W. Kunz, *Colloids Surf. A*, 2013, **427**, 95-100.

83. M. L. Klossek, D. Touraud and W. Kunz, *Green Chem.*, 2012, **14**, 2017.

84. J. Fang and R. L. Venable, *J. Colloid Interface Sci.*, 1987, **116**, 269-277.

85. Y. Gao, S. Wang, L. Zheng, S. Han, X. Zhang, D. Lu, L. Yu, Y. Ji and G. Zhang, *J. Colloid Interface Sci.*, 2006, **301**, 612-616.

86. P. Lindner and T. Zemb, *Neutrons, X-Rays and Light scattering methods applied to soft condensed matter*, Elsevier, 2002.

87. https://en.wikipedia.org./wiki/Solketal - 30.09.2017.

88. M. L. Dekker, M. Clausse, H. L. Rossano, A. Zradba, *Microemulsion Systems,Surfactant Science Ser.*, Marcel Dekker Inc., New York, 1987.

89. S. Mandl, *Paper report: Structuring of binary solvents and its impact on chemical reactivity*, Institue of Physical and theoretical Chemistry, Regensburg, 2017.

90. D. Horn, E. Lüddecke, in *NATO ASI Series* (Ed.: E. Pelizzetti), Springer Netherlands, 1996.

91. N. F. Borys, S. L. Holt, R. E. Barden, *Journal of colloid and interface science*, 1979, **71**, 526-532.

SUPPLEMENTARY MATERIAL

SOLKETAL

SpinWorks 4: Sebastian Krickl, Solketal, DMSO
rau_PROTONLF_16 DMSO {C:\Bruker\TOPSPIN2.1PL3} AK_Kunz 65

1.252
1.299

2.503

3.395

3.625

4.020

4.819

3.031
3.073

1.000

1.014
0.974

0.999

1.2
1.6
2.0
2.4
2.8
3.2
3.6
4.0
4.4

PPM

GLYCEROL

SpinWorks 4: Sebastian Krickl, Glycerol, DMSO
rau_PROTONLF_16 DMSO {C:\Bruker\TOPSPIN2.1PL3} AK_Kunz 67

2.504

3.320
3.435

4.431
4.513

2.028
1.000

PPM 0.4 0.8 1.2 1.6 2.0 2.4 2.8 3.2 3.6 4.0 4.4

OLEIC ACID

SpinWorks 4: Sebastian Krickl, Oleic acid, DMSO
rau_PROTONLF_16 DMSO {C:\Bruker\TOPSPIN2.1PL3} AK_Kunz 66

0.848

1.238

1.470

1.976

2.173

2.503

3.396

5.317

2.837

18.625

2.117

3.588

1.903

2.000

PPM

PRODUCT AFTER SOLKETAL CLEAVAGE – CRUDE MIXTURE (OIL PHASE + WATER)
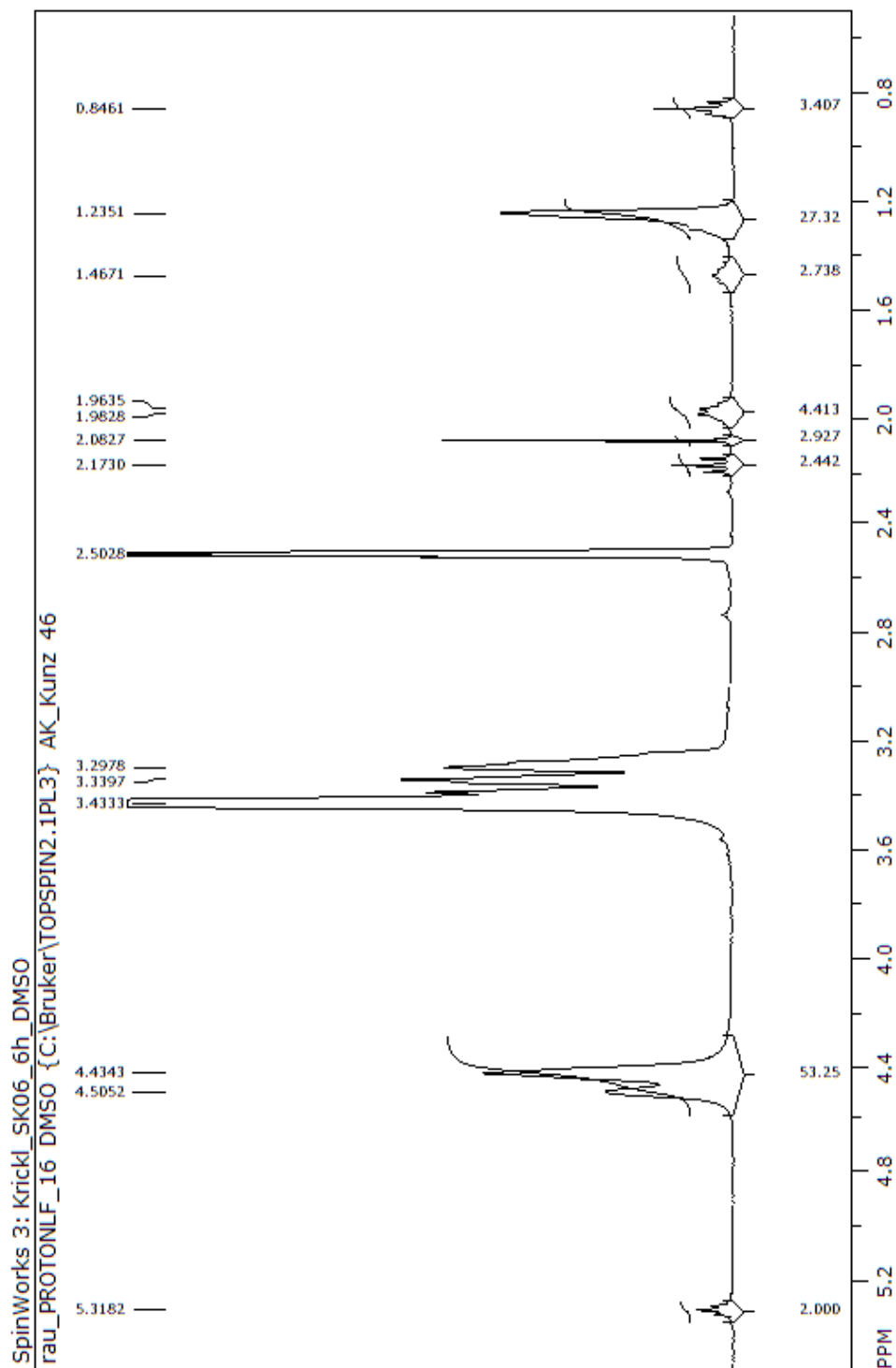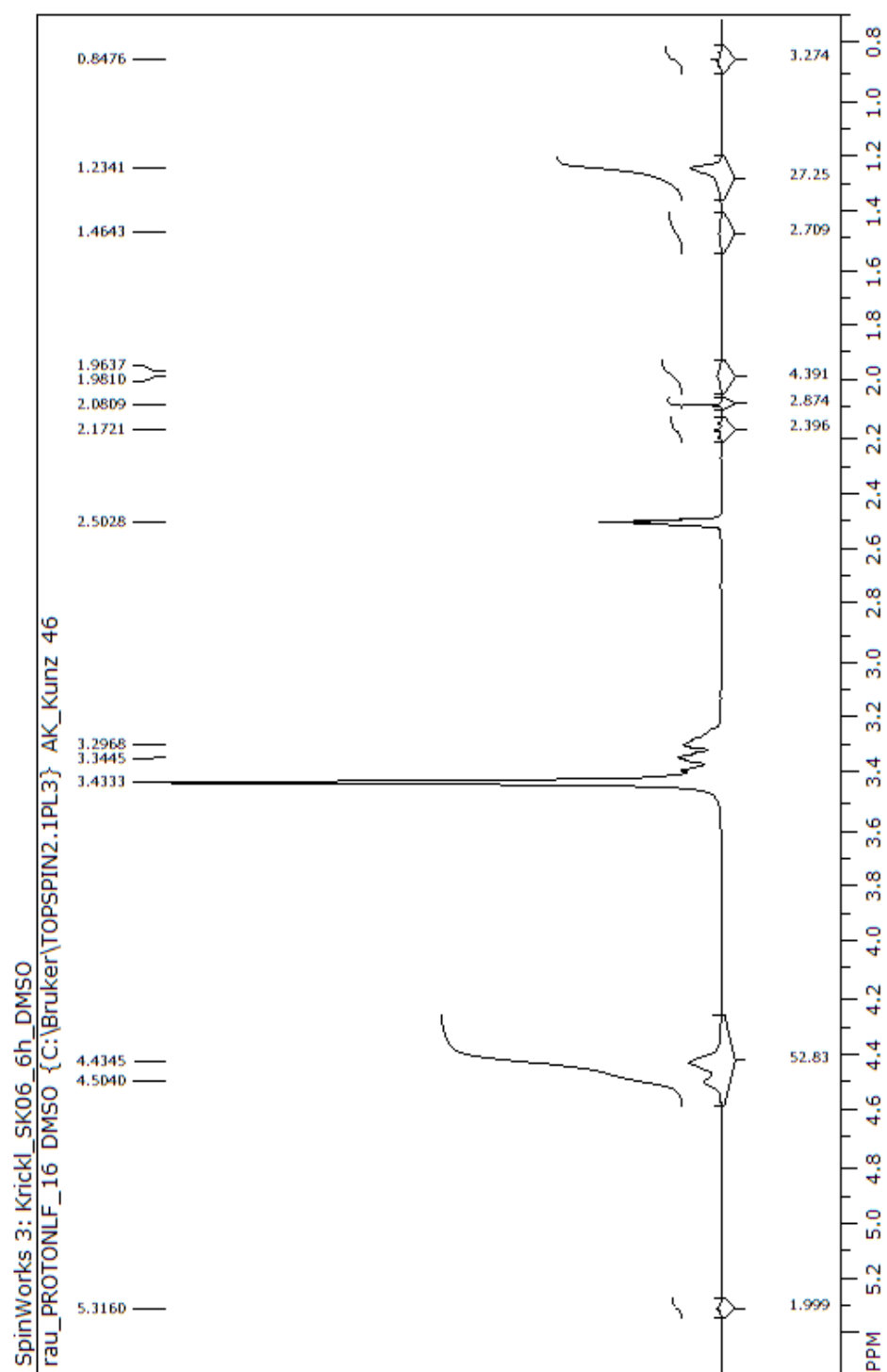
PRODUCT AFTER SOLKETAL CLEAVAGE – OIL PHASE
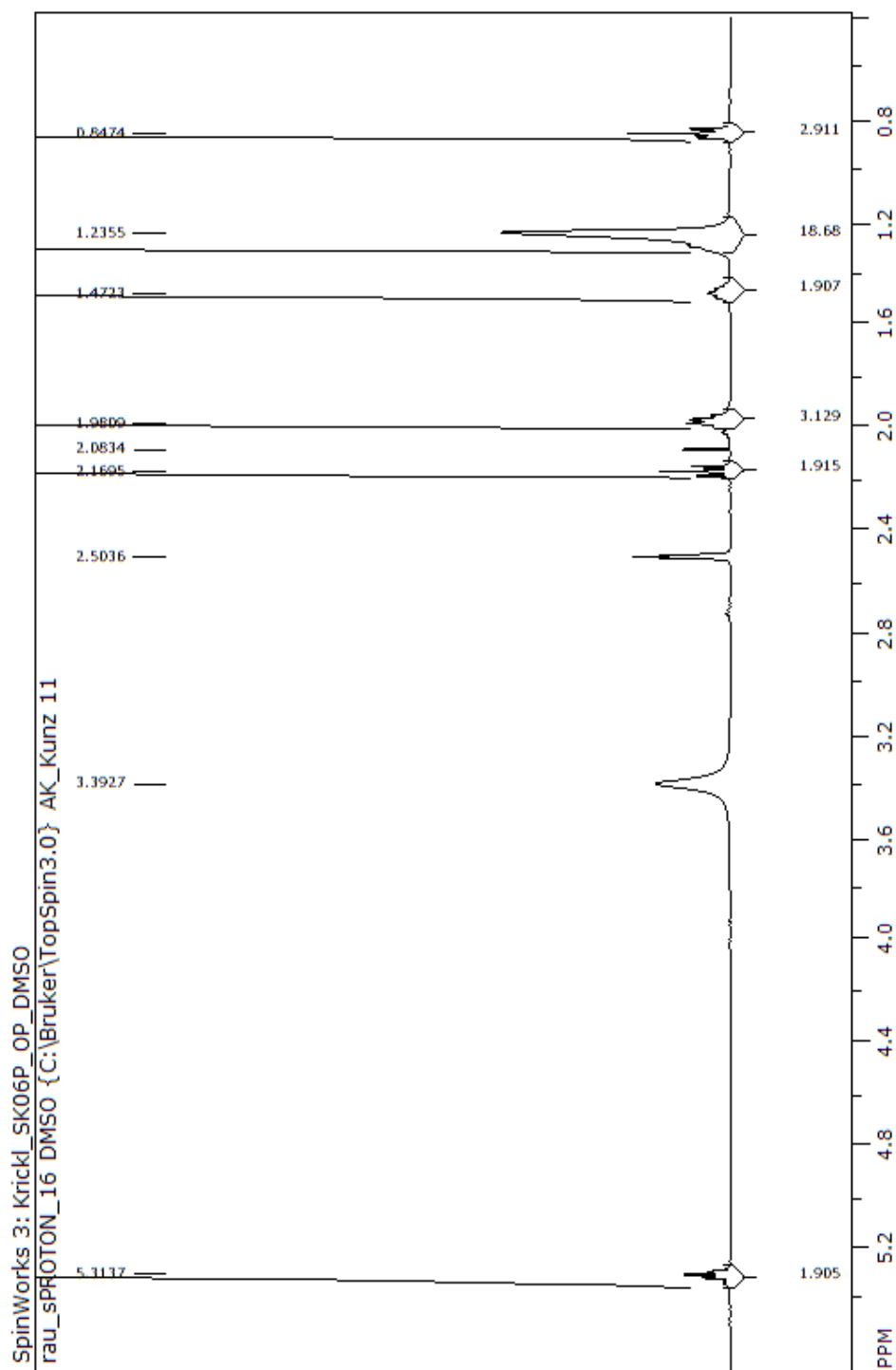
DLS POINTS FOR BENZYL ALCOHOL AND LIMONENE

- **BENZYL ALCOHOL**
  - M (Benzyl alcohol) = 108.14 g/mol
  - M (H_2O) = 18.02 g/mol

m (sample) = 3 g

EtOH

M = 46.07 g/mol

Sample	Benzyl alcohol mol%	EtOH mol%	water mol%	Benzyl alcohol wt%	EtOH wt%	water wt%
0	0	19	81	0	37.5	62.5
1	5	19	76	19.4	31.4	49.2
2	10	19	71	33.4	27.0	39.5
3	15	19	66	44.0	23.7	32.3
4	20	19	61	52.3	21.2	26.6
5	25	19	56	58.9	19.1	22.0

DMSO

M = 78.13 g/mol

Sample	Benzyl alcohol mol%	DMSO mol%	water mol%	Benzyl alcohol wt%	DMSO wt%	water wt%
0	0	14	86	0	41.4	58.6
1	5	14	81	17.5	35.4	47.2
2	1	14	76	30.5	30.9	38.6
3	15	14	71	40.6	27.4	32.0
4	20	14	66	48.6	24.6	26.8
5	25	14	61	55.2	22.3	22.4

ACN

M = 41.05 g/mol

Sample	Benzyl alcohol mol%	ACN mol%	water mol%	Benzyl alcohol wt%	ACN wt%	water wt%
0	0	3	7	0	49.4	50.6
1	5	3	65	18.4	41.8	39.8
2	1	3	60	31.9	36.3	31.9
3	15	3	55	42.2	32.0	25.8
4	20	3	50	50.4	28.7	21.0
5	25	3	45	57.0	25.9	17.1

Dioxane

M = 88.11 g/mol

Sample	Benzyl alcohol mol%	Dioxane mol%	water mol%	Benzyl alcohol wt%	Dioxane wt%	water wt%
0	0	19	81	0	53.4	46.6
1	5	19	76	15.1	46.7	38.2
2	10	19	71	26.8	41.5	31.7
3	15	19	66	36.2	37.3	26.5
4	20	19	61	43.8	33.9	22.3
5	25	19	56	50.2	31.1	18.7

TBA

M = 74.12 g/mol

Sample	Benzyl alcohol mol%	TBA mol%	water mol%	Benzyl alcohol wt%	TBA wt%	water wt%
0	0	24	76	0	56.5	43.5
1	5	24	71	15.0	49.4	35.5
2	10	24	66	26.7	43.9	29.4
3	15	24	61	36.0	39.5	24.4
4	20	24	56	43.7	35.9	20.4
5	25	24	51	50.1	32.9	17.0

THF

M = 72.11 g/mol

Sample	Benzyl alcohol mol%	THF mol%	water mol%	Benzyl alcohol wt%	THF wt%	water wt%
0	0	38	62	0	71.0	29.0
1	5	38	57	12.6	63.6	23.8
2	10	38	52	22.7	57.6	19.7
3	15	38	47	31.1	52.6	16.3
4	20	38	42	38.2	48.4	13.4
5	25	38	37	44.2	44.8	10.9

GVL

M = 100.12 g/mol

Sample	Benzyl alcohol mol%	GVL mol%	water mol%	Benzyl alcohol wt%	GVL wt%	water wt%
0	0	28	72	0	68.4	31.6
1	5	28	67	11.9	61.6	26.5
2	10	28	62	21.6	56.0	22.3
3	15	28	57	29.7	51.4	18.8
4	20	28	52	36.6	47.5	15.9
5	25	28	47	42.5	44.1	13.3

DMF

M = 73.09 g/mol

Sample	Benzyl alcohol mol%	DMF mol%	water mol%	Benzyl alcohol wt%	DMF wt%	water wt%
0	0	13	87	0	37.7	62.3
1	5	13	82	18.2	32.0	49.8
2	10	13	77	31.6	27.8	40.6
3	15	13	72	41.9	24.6	33.5
4	20	13	67	50.1	22.0	27.9
5	25	13	62	56.7	19.9	23.4

- **LIMONENE**
  - M (Limonene) = 136.12 g/mol
  - M (H_2O) = 18.02 g/mol

m (sample) = 3 g

EtOH

M = 46.07 g/mol

Sample	Limonene mol%	EtOH mol%	water mol%	Limonene wt%	EtOH wt%	water wt%
0	0	73	27	0	87.4	12.6
1	5	73	22	15.3	75.7	8.9
2	10	73	17	27.1	66.8	6.1
3	15	73	12	36.3	59.8	3.8
4	20	73	7	43.8	54.1	2
5	25	73	2	50.1	49.4	0.5

Dioxane

M = 88.11 g/mol

Sample	Limonene mol%	Dioxane mol%	water mol%	Limonene wt%	Dioxane wt%	water wt%
0	0	0	1	0	0	100
1	5	0	95	28.5	0	71.5
2	10	0	9	45.7	0	54.3
3	0.15	0	85	57.2	0	42.8
4	20	0	8	65.4	0	34.6
5	0.25	0	75	71.6	0	28.4

TBA

M = 74.12 g/mol

Sample	Limonene mol%	TBA mol%	water mol%	Limonene wt%	TBA wt%	water wt%
0	0	45	55	0	77.1	22.9
1	5	45	5	13.9	67.8	18.3
2	10	45	45	24.7	60.5	14.7
3	15	45	4	33.5	54.7	11.8
4	20	45	35	40.7	49.8	9.4
5	0.25	45	3	46.8	45.8	7.4

THF

M = 72.11 g/mol

Sample	Limonene mol%	THF mol%	water mol%	Limonene wt%	THF wt%	water wt%
0	0	78	22	0	93.4	6.6
1	5	78	17	10.3	85.1	4.6
2	10	78	12	18.9	78.1	3.0
3	0.15	78	7	26.2	72.2	1.6

GVL

M = 100.12 g/mol

Sample	Limonene mol%	GVL mol%	water mol%	Limonene wt%	GVL wt%	water wt%
0	0	70	3	0	92.8	7.2
1	5	70	25	8.4	86.1	5.5

DMF

M = 73.09 g/mol

Sample	Limonene mol%	DMF mol%	water mol%	Limonene wt%	DMF wt%	water wt%
0	0	0	1	0	0	100
1	5	0	95	28.5	0	71.5
2	10	0	90	45.7	0	54.3